NASA Contractor Report 3878

A Theory of Post-Stall Transients in Multistage Axial Compression Systems

F. K. Moore and E. M. Greitzer

GRANTS NAG3-34 and NSG-3208
MARCH 1985

NASA

NASA Contractor Report 3878

A Theory of Post-Stall Transients in Multistage Axial Compression Systems

F. K. Moore
Cornell University
Ithaca, New York

E. M. Greitzer
Massachusetts Institute of Technology
Cambridge, Massachusetts

Prepared for
Lewis Research Center
under Grants NAG3-34 and NSG-3208

National Aeronautics
and Space Administration

Scientific and Technical
Information Branch

1985

FOREWORD

In the summer of 1983, Mr. C.L. Ball arranged for the authors to spend three weeks in residence at NASA-Lewis Research Center, chiefly to consider together how to combine recent theories of surge and rotating stall. The present report describes the results of that effort. The authors would like to acknowledge Mr. Ball's assistance, and also the contribution of Mr. R. Chue of MIT who provided certain supporting calculations described in Chapter 3 of this report.

TABLE OF CONTENTS

1. INTRODUCTION

Background

Problems of compressor instability have been of concern to aircraft engine designers for a number of years, and the provision of sufficient stall margin is an important consideration in any compressor design. In addition to problems associated with the inception of stall, however, another aspect of this general topic has been of increasing import in recent years. This is the behavior of the compression system subsequent to the onset of stall, i.e., subsequent to the onset of compressor or compression system instability.

The reason for this increased interest in post-stall behavior has to do with the phenomenon of non-recoverable stall (or stall "stagnation"). In this condition (described in [1]) the hysteresis associated with compressor operation in rotating stall is large enough that, once the engine has encountered rotating stall, it cannot recover to a condition of unstalled operation. The only remedy then is to greatly decrease the engine speed to decrease the hysteresis, or, in some cases, to shut the engine down and restart it.

A key task associated with this problem is to predict post-stall behavior. This knowledge is essential for rational design of stagnation-resistant compressors. This is true not only for quasi-steady operation but also for the unsteady features of the compression system response. In the first instance, one may be able to consider the compressor in isolation, without coupling it to the system. This is essentially the problem treated by Day, Greitzer, and Cumpsty [2]

(semi-empirically), and, more recently, by Moore [3] in a rather more fundamental manner. To grapple with the actual situation in more generality, however, one must deal with the unsteady behavior of the compressor during the mass flow oscillations that characterize post-stall transients. This involves a description of the possible formation (growth) in the compressor of a rotating stall cell during this period, while at the same time, the compressor interacts with other components of the system.

It is to be stressed from the outset that this task cannot today be carried out by exact or numerical solution of the basic partial differential equations of fluid motion. The prediction of even steady-state rotating stall performance has not yet been carried out on this level. However, many of the salient features of rotating stall have been predicted using certain simplifying assumptions, in a theory by Moore [3]. We do not hope to unravel all of the issues connected with this flow regime, but it is nevertheless felt that a useful model for transient compressor operation can be formulated in a similar way. This will not only be helpful for general physical insight, but should give guidance to experimental studies, and also illustrate some of the overall effects of different design parameters. This report, which essentially covers the work done by the authors during the period 7/25/83 to 8/12/83 while both were in residence at NASA Lewis Research Center, describes an approximate theory of this type.

Motivation: Time Scales in Transient Compressor Operation

Before plunging into the details of the analysis, it seems appropriate to provide a motivating discussion of the physical situation. This is

perhaps especially true in view of the large amount of work that has been done on dynamic behavior of compressors and compression systems. In this section, therefore, we will present some basic physical arguments that underlie an examination of the problem under consideration; that is, combined surge and rotating stall. In particular, we will show that there appears to be a strong reason for an examination of the transient behavior of the compressor as it passes in and out of rotating stall, since its behavior can affect the overall system response.

One way to do this is to consider the time scales that are associated with the phenomena that occur during the transients of interest. The first of these is the rotating stall formation time. This is the time needed for the flow in the compressor to change from a nominally uniform (unstalled) to a severely asymmetric (rotating stall) state. This change can be associated with the shedding of the bound circulation of a significant portion of the blading in the compressor (say, one-third to one-half) and the subsequent convection of this shed vorticity downstream on the order of the circumference. The time taken for this to occur might thus be on the order of the flow time for this distance, i.e., $\pi D/C_x$ where D is the diameter of the compressor and C_x is some representative axial velocity.

The above argument suggests the use of $\pi D/C_x$ as the proper rotating stall formation time. In the past, however, this time has been quoted in terms of rotor revolutions, i.e., in terms of $\pi D/U$ where U is the blade speed. While perhaps not as physically grounded as $\pi D/C_x$, available data is in terms of this latter parameter. Also, once a given compressor is

specified, the axial velocity and the rotor speed are of similar magnitudes, linked by geometry. Thus we will defer to this convention and specify

$$\text{Rotating stall formation time scale} = \tau_R = \pi D/U \tag{1.1}$$

as the time scale for rotating stall cell formation. Available data indicates that the characteristic time is roughly two rotor revolutions and that the time to "fully develop" is even longer, being several characteristic times.

Another relevant time scale is the "flow change time." This is the characteristic time for changes in the overall (annulus averaged) mass flow through the compressor. It is set by a balance between the pressure forces that are available to accelerate the flow in the compressor duct during a stall transient and the inertial forces that arise from this acceleration.

If the overall compressor pressure rise is ΔP and the pre-stall axial velocity is denoted by C_x then this balance of pressure and inertial force yields

$$\rho \frac{L_c C_x}{\tau_c} \sim K\Delta P \tag{1.2}$$

where $K\Delta P$ is a number of order unity. In this expression the quantity L_c is the effective length of the compressor duct and τ_c is the flow change time. We can write this in terms of non-dimensional compressor parameters $\phi (= C_x/U)$ and $\psi (= \Delta P/\rho U^2)$ to yield an expression for the flow change time scale as

$$\text{Flow change time scale} = \tau_c = \frac{L_c}{U}\frac{\phi}{K_\psi} = Z\frac{L_c}{U} \tag{1.3}$$

In this expression Z is a non-dimensional number that is a function of the compressor parameters. Z is expected to be of order magnitude unity.

A third time scale is the "Helmholtz resonator time." This is the characteristic time for small oscillations in a compression system, considered as a Helmholtz resonator. Using the formula for the Helmholtz frequency, ω_H, this is

$$\text{Helmholtz resonator time scale} = \tau_H = \frac{1}{\omega_H} = \frac{1}{a_s}\frac{V_p L_c}{A_c} \tag{1.4}$$

where V_p is the system plenum volume and A_c is the through-flow area of the compressor.

For low speed machines or for compressors of few stages, the large amplitude (surge) system oscillation time scale may also be of this order so that it and the flow change time will be roughly the same. However, for multistage machines, especially at high speed, the transients that occur subsequent to stall are not at all sinusoidal, but are rather of the nature of relaxation oscillations. Hence the flow change time scale and the Helmholtz resonator time scale can be quite different. (Note that for the relaxation type of transient, the plenum pressure change during the transient is small because the transient is so rapid. Thus the actual plenum volume should not enter into the definition of this time scale.)

There is also a fourth time scale which we also include for completeness. This is the "plenum emptying time." It is only

appropriate to the relaxation type of oscillation, as it is set by a balance between resistive and capacitive elements, i.e., between flow resistance in the throttle and the pressure difference (plenum to atmosphere) due to the storage of potential energy of compression of the gas in the plenum. It can be much longer than the flow change time and is the principle part of the period of surge cycles experienced by multistage compressors near design speed. Explicitly this time is given by:

$$\text{Plenum emptying time} = \tau_e = \frac{\psi}{\phi}\frac{U}{a_s}\frac{V_p}{a_s A_c} = E\left(\frac{U}{a_s}\right)\frac{V_p}{a_s A_c} \tag{1.5}$$

It is useful to put the foregoing times into non-dimensional ratios. These will contain not only the non-dimensional numbers Z and E introduced above, but two other non-dimensional parameters as well. These are:

$$B = \frac{U}{2\omega_H L_c} = \frac{U}{2a_s}\sqrt{\frac{V_p}{A_c L_c}} \tag{1.6}$$

which has been described in detail in [3] and [4], and

$$\ell_c = \frac{2L_c}{D} \tag{1.7}$$

the ratio of compressor effective length to radius.

The non-dimensional ratios of the various time scales are thus:

$$\frac{\text{Helmholtz resonator time}}{\text{Rotating stall formation time}} = \frac{\tau_H}{\tau_R} = \frac{B\ell_c}{\pi} \tag{1.8}$$

$$\frac{\text{Flow change time}}{\text{Rotating stall formation time}} = \frac{Z\ell_c}{2\pi} \tag{1.9}$$

$$\frac{\text{Plenum emptying time}}{\text{Rotating stall formation time}} = \frac{2B^2}{\pi} E\ell_c \tag{1.10}$$

If one substitutes representative numbers into the above non-dimensional ratios, it becomes evident that the first two at least are roughly of magnitude unity. In other words, in practical circumstances the rotating stall cell formation time is of the same order as the mass flow change time. This is the central point of this discussion concerning time scales.

The implication of this rough parity (between the time scale of rotating stall cell formation and the time for a significant change in the overall mass flow during a transient) is that rotating stall will not have time to fully form during this type of non-steady flow. This has significant implications in turn for the modelling of post-stall transients, since, during the transient, the compressor is not performing in a quasi-steady manner. Thus, information obtained from a steady-state compressor test with the machine operating in rotating stall may not be at all representative of the performance during a rapid post-stall transient. If so, it is imperative to address the question of compressor behavior during these transients. Specifically, the theory developed herein must include an assessment of how the growth or decay of rotating stall affects the instantaneous compressor pumping characteristic, and hence overall system behavior.

Before leaving the discussion of time scales, there is one further point that should be mentioned. The principle aspect of compressor unsteady response that we are examining is that associated with the growth of an asymmetric flow pattern which has a length scale on the order of the compressor diameter. The time scale is thus very much longer than that

associated with the unsteady response of a single blade passage. This latter might be on the order of the through-flow velocity, W, divided by b, the blade chord, and hence the ratio of the blade response time to the rotating stall formation time is of order

$$\frac{\text{Blade through flow time}}{\text{Rotating stall formation time}} \sim \frac{b/W}{\pi D/U} = \frac{b}{\pi D}\frac{U}{W} << 1 \qquad (1.11)$$

Thus, the precise modelling of the unsteady performance of the blades, per se, would not be expected to be a key ingredient of a theory of stall-cell growth.

Overall Format of the Report

In the next section we discuss the physical assumptions inherent in the compressor and compression system models that we will use. We then briefly describe separately the two "components" of the overall problem, rotating stall and surge. An analysis is first presented of rotating stall (where the annulus averaged flow is constant in time, but the flow is non-uniform around the circumference). The pure surge mode (in which the annulus averaged mass flow varies with time, but the flow is uniform around the circumference) is then examined. Approximate solutions are developed for both of these modes.

Following these two sections, which are to some extent reviews of previous work that the present analysis builds on, the combined problem is introduced. Using an approximate (Galerkin) procedure, a set of coupled nonlinear equations is derived which describes the time varying state of the system. The nature of the equations is discussed, and then certain numerical solutions are described which show the effects of certain parameters of interest. Finally, some comments are made about future avenues of research, both theoretical and experimental, that are thought to be needed for this general problem.

2. FLUID DYNAMIC MODEL

The basic compression system to be analyzed is shown in Figure 2.1. The coordinate system that will be used, and the directions of the different velocity components, as well as all the different axial stations that we will employ, are also indicated.

The system consists of a compressor operating in a duct and discharging to a downstream plenum. The plenum dimensions are large compared to those of the compressor duct so that the velocities and fluid accelerations in the plenum can be considered negligible. Hence the pressure in the plenum can be considered to be uniform spatially, although varying in time. The flow through the system is controlled by a throttle at the plenum exit.

The systems that we consider will have overall pressure rises, atmosphere to plenum, that are small compared to the ambient level. If, also, we assume Mach numbers to be small, and oscillations to have frequencies well below those of acoustic resonance, then we can adopt an incompressible flow description of compressor behavior (although, of course, compressibility is important in setting system dynamics). The basic compression system model, as discussed so far and shown in Figure 2.1, has been used by many investigators. Where we depart from previous practice in analysis of compression system transients, however, is in the coupling of an analysis of the two-dimensional unsteady flow in the compressor with the lumped-parameter system model. We therefore should also briefly describe our representation of the compressor.

The basic compressor model is similar to that presented in [3]. The

compressor is considered to have a high hub/tip radius ratio, so that a two dimensional description can be used. The compressor duct is modeled as having an inlet section (contraction) followed by a constant-area section upstream of the compressor. The annulus immediately downstream of the compressor also has constant area. These restrictions simplify the analysis, but could be removed in a more general treatment.

The following nomenclature will be used (see Figure 2.1): all distances will be non-dimensionalized by the mean radius. The non-dimensional circumferential and axial coordinates and time are:

Circumferential coordinate: $\theta = \dfrac{\text{circumferential distance}}{R}$ (2.1)

Axial coordinate: η = axial distance/(R) (2.2)

Time: $\xi = Ut/R$ (2.3)

As discussed in [3], the basic model we adopt for the unsteady performance of a compressor blade row is that the pressure rise across a single row is given by

$$\frac{\Delta P}{\frac{1}{2}\rho U^2} = F(\phi) - \tau \frac{d\phi}{dt} \tag{2.4}$$

where $\phi (= C_x/U)$ is the axial velocity coefficient at the compressor. The quantity $F(\phi)$ is the axisymmetric performance characteristic, and τ can be viewed as a "time constant" associated with the internal lags in the compressor. In [3], it was shown that a reasonable value for τ is roughly $\tau \sim 2b_x/C_x$.

The unsteadiness in the flow through a stator passage reflects the accelerations associated with transient effects. For a rotor, however,

there is another source of the unsteadiness seen by a blade row due to the rotor blades moving (with velocity U) through a circumferentially non-uniform flow. Therefore,

$$\left(\frac{d\phi}{dt}\right)_{\text{stator}} = \frac{\partial\phi}{\partial t} = \frac{U}{R}\frac{\partial\phi}{\partial\xi} \tag{2.5}$$

$$\left(\frac{d\phi}{dt}\right)_{\text{rotor}} = \frac{\partial\phi}{\partial t} + \frac{U}{R}\frac{\partial\phi}{\partial\theta} = \frac{U}{R}\left(\frac{\partial\phi}{\partial\xi} + \frac{\partial\phi}{\partial\theta}\right) \tag{2.6}$$

We note that in the present situation, because of the possibility of growth or decay of velocity non-uniformities, there is not necessarily Galilean equivalence between the changes in time and the spatial derivatives, as there would be for a pure traveling wave.

Proceeding to the multistage situation, we have to give the pressure rise across an N-stage compressor (not including the inlet and exit guide vanes which we will discuss subsequently):

$$\frac{\Delta P}{\rho U^2} = NF(\phi) - \frac{N\tau U}{2R}\left(2\frac{\partial\phi}{\partial\xi} + \frac{\partial\phi}{\partial\theta}\right) \tag{2.7}$$

Rather than introduce more of the detailed features of the model at this point, we will next examine the two special cases that were mentioned previously, with discussion of further aspects of the model being introduced as needed. Since the development of the pure surge and rotating stall situations have appeared elsewhere, however, we will not present the derivation ab initio, but rather refer the reader to [3], [4], [5], and [6] for fuller accounts.

3. ROTATING STALL ANALYSIS

Governing Equation for Rotating Stall (Constant annulus averaged mass flow)

We begin with the equation governing a disturbance (g) of axial flow coefficient (ϕ)

$$\phi = \Phi + g \tag{3.1}$$

where Φ is the steady mean flow coefficient (or nondimensional axial velocity) and g is the nonaxisymmetric disturbance. This nonaxisymmetric part of the axial velocity will be a function of θ^*, where $\theta^* = \theta - f\xi$. That is, θ^* is measured in a coordinate system traveling with the stall cell, which propagates around the circumference with a nondimensional, constant speed f. (The physical speed in the laboratory coordinate system is fU.)

Equation (1) of Part III of [3] is

$$\lambda\frac{dg}{d\theta^*} - mfh + \Psi - \psi_c(\phi) = 0 \tag{3.2}$$

where h is the nondimensional circumferential velocity distrubance. Like g, h is also a function of θ^*. The quantity m is a parameter which reflects inlet and outlet flow inertia effects. If the exit flow is a sudden expansion, and entrance flow is potential, then m = 1. If the exit is a straight duct, we know only that m = 2 for small disturbances. We assume that m is constant for large disturbances as well, with m = 2 being appropriate for long diffusers. The parameter λ depends on f and a, the latter being a dimensionless expression of the time lag (τ) of pressure rise for a single blade passage, as described in [3].

$$\lambda \equiv \frac{1}{a}\left(\frac{1}{2} - f\right) \tag{3.3}$$

$$a \equiv R/(UN_T) \tag{3.4}$$

The quantity a is assumed known while f (and hence λ) is to be found as an eigenvalue of the solution.

It is emphasized in [3] that although the compressor characteristic function $\psi_c(\phi)$ is assumed known, it must be identified as an "axisymmetric characteristic," applicable when there is no rotating stall. The actual steady pressure-rise coefficient (Ψ) produced when the compressor is in rotating stall* differs from $\psi_c(\phi)$ because there is a nonlinear effect of rotating stall itself. That is, even when $\phi = \Phi$ (the average flow coefficient), Ψ and ψ_c differ. We denote that difference by δ:

$$\delta \equiv \Psi - \psi_c(\Phi) \tag{3.5}$$

so the last two terms of Eq. (3.2) are

$$-[\psi_c(\phi) - \psi_c(\Phi)] + \delta \equiv -G(g) + \delta \tag{3.6}$$

and the quantity in brackets, depending only on $\phi-\Phi$, or g, we write as G(g). These relationships are illustrated on Fig. 3.1. Equation (3.2) may now be written

$$\lambda\frac{dg}{d\theta^*} - mfh - G(g) + \delta = 0 \tag{3.7}$$

It is necessary to specify how $h(\theta^*)$ and $g(\theta^*)$ are related before proceeding to solve Eq. (3.7).

---

*This would be the coefficient measured during a steady-state compressor test.

The "$dh/d\theta^* = -g$" Approximation

The relation between h and g is discussed in Appendix A of [4]. In general, complete flow field solutions in the entrance and exit regions are needed to relate h and g, and no simple exact relationship applies except in special cases. In [3] and [4] arguments are given, however, to support the adoption of the approximate relation

$$\frac{dh}{d\theta^*} = -g \tag{3.8}$$

Some further discussion of this point is also presented in Appendix A of the present report. The general conclusion from these discussions is that the approximation can be adopted for the nonlinear stall cell calculation with some confidence. We will therefore do this in the remainder of the report.

If this is done, the set of equations that describe pure rotating stall can be written by introducing Eq. (3.8) into the derivative of Eq. (3.7) to yield

$$\lambda\frac{d^2g}{d\theta^{*2}} - \frac{dG}{dg}\frac{dg}{d\theta^*} + mfg = 0 \tag{3.9}$$

The axial velocity perturbation, g, is also required to be periodic with period 2π.

$$g(\theta^* + 2\pi) = g(\theta^*) \tag{3.10}$$

The cyclic integral of h is required to vanish, in order that the transverse velocity disturbance introduces no circulation.

$$\int_0^{2\pi} h d\theta^* = 0 \tag{3.11}$$

The condition given in Eq. (3.11) is strictly valid only when the entrance flow is potential. Further research will be needed to explore conditions alternative to Eq. (3.11). In view of Eqs. (3.10) and (3.11), integration of Eq. (3.9) over a full cycle yields the performance effect of rotating stall:

$$\delta = \frac{1}{2\pi} \int_0^{2\pi} G(g) d\theta^* \tag{3.12}$$

Equations (3.9), (3.10), and (3.12) will represent the basic rotating-stall problem: a given throttle setting defines the origin of g and allows the given axisymmetric characteristic to be expressed (relative to the throttle point) as the function G(g). Then, the eigensolution $g(\theta^*)$ is found by integrating Eq.(3.9) with f (and hence λ) found as an eigenvalue to fix the period at 2π. The nonlinear performance effect then follows from Eq. (3.12).

Numerical Solution for a Cubic Characteristic

In Refs. [7] and [8] it is argued that the axisymmetric characteristic is typically a smooth S-shaped curve. (In those references, the axisymmetric curve is estimated for a three-stage compressor using a procedure based on corrections to transient data.) If this idea is correct, a physically realistic function would be a simple cubic, as that shown in Fig. 3.2. We might therefore expect that the in-rotating-stall characteristic calculated using the cubic will be a good representation of that calculated using an exact axisymmetric diagram.

The formula for the particular curve shown in Fig. 3.2 is

$$\psi_c(\phi) = \psi_{c_o} + H\left[1 + \frac{3}{2}\left(\frac{\phi}{W} - 1\right) - \frac{1}{2}\left(\frac{\phi}{W} - 1\right)^3\right] \tag{3.13}$$

We locate the throttle-line intersection at a point β to the right of the midpoint of the diagram. Since we chose to measure ϕ from the minimum of ψ_c (representing the shut-off condition in this case), and since G and g are both measured from the throttle-line intersection,

$$G \equiv \psi_c(\phi) - \psi_c(W + \beta) \tag{3.14}$$

$$g \equiv \phi - (W + \beta) \tag{3.15}$$

Substituting into Eq. (3.21) yields

$$G(g) = \frac{1}{2}\frac{H}{W}\left[3\left(1 - \frac{\beta^2}{W^2}\right)g - 3\frac{\beta}{W^2}g^2 - \frac{1}{W^2}g^3\right] \tag{3.16}$$

which we will use hereafter to represent the damping function G(g).

In Refs. [7] or [8], a numerical procedure is presented for solving Eqs. (3.9) to (3.12), and as part of the present study, R. Chue of MIT carried out calculations for a particular cubic G(g). The value used for m was 1.75. H and W were chosen so that the cubic would have the same peak and valley points as the actual curve; their values were 0.18 and 0.25 respectively. Rather than Eq. (3.3), a somewhat more elaborate relation between λ and f was used, in which guide-vane effects were included, following Ref. [8]. Numerically, the relation was, in effect,

$$\lambda = 4.34(0.378 - f)$$

Figure 3.3 shows how f increases when the throttle is opened (i.e., as β is increased), as predicted in [3]. Figs. 3.4a-f show how the axial

velocity disturbance $g(\theta^*)$ evolves as the throttle is opened. When $\beta = 0$, the symmetry features shown in Fig. 3.4a must occur, and we note that $g(\theta^*)$ swings between extremes which lie on the unstalled and reverse-flow legs of the characteristic. As β increases, these extrema remain nearly the same, but more time is spent unstalled, so to speak. There is no solution beyond $\beta = 0.25$, which corresponds to the peak point of the curve.

The most interesting result is shown in Fig. 3.5. There, the cubic axisymmetric characteristic is shown with the calculated δ superposed to form the predicted in-stall, pressure-rise variation with throttle setting (Φ). The graph dramatically illustrates the idea of Ref. [7], that the usually-observed sudden break in performance at the stall point, and subsequent drop into "deep stall" as the throttle is closed, is the result of being in rotating stall, rather than a direct effect of the inherent axisymmetric characteristic of the compressor. The latter might, in fact, be quite smooth and gradual, with no break at all.

Approximate Solution Using Galerkin Procedure

Because we shall be concerned with the analysis of complicated oscillations of which rotating stall will be only a special case, it is useful, at this initial stage of the investigation, to devise a simple method of analytically representing rotating stall alone, with the idea of then using it later for more general post-stall disturbances. If the damping function $G(g)$ is smooth, the Galerkin method of nonlinear mechanics (Ref. [9]) is perhaps appropriate. (In this connection we note that this technique has been used quite successfully for the van der Pol problem, which is just the symmetric version of the present situation with $\beta = 0$.)

In general, in this procedure, the solution to the differential equation is represented by a suitable sequence of basic functions. If the functions are well chosen, and enough terms in the sequence are taken, the "true" solution can be represented very accurately. Fourier series or spectral methods are special cases of this procedure.

We are seeking, for present purposes, the simplest possible wave representation capable of describing the stall phenomena. We have thus taken the somewhat drastic step of truncating the sequence after one harmonic term; in effect, a single term Galerkin procedure. The form chosen for g is therefore

$$g \propto \sin \theta^*$$

For the present exploratory purposes, this approximation will prove to be reasonable. However, it is very important to be clear about the limitations of this approximation. The single-term Galerkin procedure is most accurate for weakly nonlinear systems. The present set of equations is strongly nonlinear. Thus, although it will turn out that the approximation for g, the axial velocity disturbance, is reasonable, as are the pressure rise curves, which are averaged functions of g, the method does not give a good description of the derivatives of g. This is to be expected since the oscillations represented by Eq. (3.9) with small λ would be of the relaxation type, and it would need many more than one harmonic to describe the shape accurately.

In this study, we wish to emphasize the amplitudes of disturbances and integrated effects on performance. Thus, the information that is of most interest at present is just that information which is least sensitive to

the higher harmonics of the stall-cell description. Hence, for our purposes, the single-term approximation should be adequate, and should lead to a compact description of the overall stall behavior. Appendix B gives some results obtained using a two-term sequence of functions, as well as some additional discussion on the effects of incorporating more of the complete set of the basic functions.

We now take g to be of the specific form

$$g = A^*W \sin\theta^* \ . \tag{3.17}$$

Substituting into Eqs. (3.7, 3.16) yields

$$\frac{1}{W} L(\theta^*) = (-\lambda + mf)A^*\sin\theta^* - \frac{3H}{2W}\left[(1-\beta^2/W^2)A^* - (1/4)A^{*3}\right]\cos\theta^* \tag{3.18}$$

If the equation were satisfied exactly, the residual $L(\theta^*)$ would be 0. It is not, and $L(\theta^*)$ represents the error involved. In keeping with the Galerkin procedure, we require that the $\sin\theta^*$ and $\cos\theta^*$ moments of $L(\theta^*)$ vanish. This yields expressions for stall-cell speed (f) and wave amplitude (A^*):

$$\lambda = mf \tag{3.19}$$

and

$$A^* = 2(1 - \beta^2/W^2)^{1/2} \tag{3.20}$$

The form of g is thus

$$g = \left[2W(1 - \beta^2/W^2)^{1/2}\right] \sin\theta^* \tag{3.21}$$

Note that in the one-harmonic solution, there is no question as to the $dh/d\theta' = -g$ approximation, because only a single term is used.

Equation (3.21) can be substituted into Eqs. (3.12, 3.17) to give the

result for δ

$$\delta = -3H(\beta/W)\ (1 - \beta^2/W^2) \tag{3.22}$$

Hence, according to Eq. (3.5) the rotating stall performance is

$$\Psi = \psi_{c_o} + H\left(1 - \frac{3}{2}\frac{\beta}{W} + \frac{5}{2}\frac{\beta^3}{W^3}\right) \tag{3.23}$$

where we recall that the parameter β represents the effect of the throttle setting, as shown on Fig. 3.2. This last formula can be compared with the axisymmetric characteristic (Eq. (3.13)):

$$\psi_c = \psi_{c_o} + H\left(1 + \frac{3}{2}\frac{\beta}{W} - \frac{1}{2}\frac{\beta^3}{W^3}\right) \tag{3.24}$$

Comparison with numerical solution. Equation (3.24) has already been indicated on Figs. 3.2 and 3.5. On Fig. 3.5 we also show Eq. (3.23), which may be compared with the exact result. Although the two curves do not agree numerically, it is remarkable that the qualitative features of the performance effect are well predicted by the simple, first-harmonic theory, especially the steep rise near $\beta = W$, and the equally steep drop near $\beta = -W$.

Figure 3.6 shows the amplitude of the disturbance as a function of β/W. It vanishes at the two extremes of the diagram, $\beta = \pm W$, and has its greatest value (2W) at the midpoint, $\beta = 0$. Although it is satisfying that "recovery" (in the sense of a limiting throttle setting) at $\beta = W$ is very nearly correct, it is to be noted that the manner in which this occurs is different than in the numerical solution. For the single term approximation, the amplitude of the disturbance vanishes, while in the numerical

solution, the amplitude of the disturbance stays quite constant as the width of the reversed-flow region decreases. The one-harmonic solution is displayed on Figs. 3.4a,e to show the differences. Obviously it is impossible for the simple harmonic wave to represent the sudden drop into, and recovery from, reversed flow which occurs when β is near W, consistent with our previous remarks about the strengths and weaknesses of the approximate method. We will return to this topic when we discuss the combined surge and rotating-stall results.

To summarize, the foregoing discussion of pure rotating stall, as well as the results in Appendices A and B, support the following conclusions regarding the method of analysis to be applied in the more complex combined situation:

(1) The approximate relation $dh/d\theta^* = -g$ seems to be a valid one, although no direct proof yet exists. It is also consistent with the one-term representation of the solution, and it will be used throughout the rest of this report.

(2) A single harmonic Galerkin method is also a useful approximation. It correctly forbids any solution beyond the stability limits of the compressor characteristic, and it gives a qualitatively correct picture of the nonlinear effect of rotating stall on performance. However, it cannot represent the relaxation type of transition which arises in fully developed rotating stall, nor can it show effects of diagram steepness. These deficiencies are perhaps not serious for the early stages of development of a rotating stall transient. In any case, no analytical improvement has been found, and we shall adopt the single-harmonic Galerkin method for the

remainder of this study.

(3) The underlying compressor characteristic for this study is the axisymmetric one which, as Fig. 3.5 shows, is quite different from that one would measure during rotating stall. Accepting the arguments of Ref. [7], we adopt a smooth curve, of which the cubic is a very good model, to represent the axisymmetric characteristic. Its only shape parameter is its steepness, H/W.

4. SURGE ANALYSIS

Governing Equations for Pure Surge

We turn now to the situation when axial flow coefficient is constant around the annulus (not a function of θ), but varies with time t. In effect, we replace Eq. (3.1) by

$$\phi = \Phi(t) \tag{4.1}$$

The time-dependence of Φ represents surge. As explained and analyzed in Refs. [5] and [6], the surge phenomenon depends not only on the compressor and its connecting ducts, as rotating stall does, but also on the system to which the compressor connects.

The governing equations (from Ref. [5]) may be expressed as the following pair; the first represents momentum and the second, mass conservation:

$$\ell_c \frac{d\Phi}{d\xi} + \Psi(\xi) - \psi_c(\Phi(\xi)) = 0 \tag{4.2}$$

$$\ell_c \frac{d\Psi}{d\xi} - \frac{1}{4B^2}\left[\Phi(\xi) - \sqrt{\frac{2}{K_T}\Psi(\xi)}\right] = 0 \tag{4.3}$$

Equation (4.3) assumes a parabolic throttle characteristic, K_T; if the throttle can be considered linear, then (bars represent mean values)

$$\ell_c \frac{d\Psi}{d\xi} - \frac{1}{4B^2}\left[\Phi(\xi) - \bar{\Phi} - \frac{1}{k_T}(\Psi(\xi) - \bar{\Psi})\right] = 0 \tag{4.4}$$

replaces Eq. (4.3). The dimensionless time and the nondimensional effective length of the compressor and its ducting are defined as:

$$\xi = Ut/R \; ; \quad \ell_c = L_c/R \tag{4.5}$$

Equation (4.3) also implies that the inertia in the throttle duct has been neglected. This is generally a very good assumption, because throttle

slopes are commonly steep, throttle mass excursions are small, and throttle lengths are usually short compared to compressor lengths.

The nondimensional parameter B, defined in Eq. (1.6), will play an important role in the combined problem, as well as in the pure surge case. This parameter can be regarded as a measure of the ratio of pressure forces to inertial forces for a given rate of mass flow change. High values of B thus tend to be associated with system oscillations (surge) while low values tend to lead to rotating stall, i.e., operation at a stable system equilibrium operating point.

Without carrying out any detailed calculations the role of the different parameters and variables can perhaps be seen most readily if we combine Eqs. (4.2) and (4.4) to give the familiar form of a second degree ordinary differential equation. This can be regarded as an equation describing the behavior of a nonlinear mass/spring/damper system and is:

$$\frac{d^2\Phi}{d\xi^2} + \frac{1}{\ell_c}\left(\frac{1}{4B^2k_T} - \frac{d\psi_c}{d\Phi}\right)\frac{d\Phi}{d\xi} + \frac{1}{4\ell_c^2B^2}\left[(\Phi - \bar{\Phi}) - \frac{\Psi - \bar{\Psi}}{k_T}\right] = 0 \qquad (4.6)$$

Several points can be seen from Eq. (4.6). First, it is clear that the main part of the "damping" in this system is due to the axisymmetric compressor characteristic. The role of the B parameter can be seen to affect not only the damping (varying the B parameter can change negative to positive damping) but also the stiffness, or restoring term. Finally, even though this equation is similar in some respects to that which governs rotating stall, one should note that the coefficients are different, and the independent (time-like) variable is different, because the basic

some respects to that which governs rotating stall, the coefficients are different, the independent variable (time) is different, and the basic physical situation being described is different.

We will not belabor the discussion of the basic equations that apply to pure surge, since these have been examined in detail in [8] and [9]. The two main points that we wish to emphasize as being of importance for this study, however, are:

(1) A compression system consisting of compressor, plenum, and throttle is sufficiently general to exhibit surge as well as rotating stall. It is therefore presumably adequate for our initial explorations of the combined transients, although the ultimate interest is in the development of more accurate models of entire engines.

(2) The axisymmetric characteristic which governs pure rotating stall also governs pure surge, in both cases providing the damping effect (which can be either positive or negative) of the oscillation. We will find the same situation in modelling the combined rotating stall/surge problem.

5. DERIVATION OF EQUATIONS FOR GENERAL SYSTEM TRANSIENT

Pressure Balance of a Compressor

We turn now to the analysis of oscillations of the compression system which are neither pure surge nor pure rotating stall. We expect that such motions, which were discussed in the previous two sections, should fall out as special cases of the system we will now derive.

An overall sketch is provided in Fig. 2.1. An irrotational, inviscid flow is imagined to proceed from an upstream (atmospheric) reservoir at stagnation pressure p_T through an entrance duct to the IGV entrance at 0. We suppose that ϕ, the axial flow coefficient there, can depend on both angle θ around the wheel and time t, although the reservoir pressure is constant. As a result of the flow process in the approach duct, if ϕ varies with θ, then a circumferential velocity coefficient $h(\xi,\theta)$ must be present at the IGV entrance. It should be noted that the present coordinate system is fixed in the laboratory, whereas in Section 3 above (as in Refs. [3] and [4]), the system traveled with a supposed permanent rotating stall pattern.

The following averages may be defined:

around wheel:
$$\frac{1}{2\pi}\int_0^{2\pi} \phi(t,\theta)d\theta \equiv \Phi(t) \tag{5.1}$$

over long time:
$$\frac{1}{T}\int_0^{T} \Phi(t)dt \equiv \overline{\Phi} \tag{5.2}$$

We recall (Eqs. (2.2, 2.3) that time is measured in radians of wheel movement and distance, both circumferentially and axially, in wheel radii.

Proceeding just as in Refs. [3] and [4], we suppose that any

circumferential non-uniformity within the compressor must, by a continuity argument and by evidence cited in Ref. [2], go straight through the machine. That is, corresponding to Eq. (3.1), we write

$$\phi = \Phi(\xi) + g(\xi,\theta) \; ; \quad h = h(\xi,\theta) \tag{5.3}$$

and note that, by definition, the angle-averaged g must vanish. Also, because no circulation can arise in the entrance duct, h must have vanishing average as well. Thus,

$$\int_0^{2\pi} g(\xi,\theta)d\theta = 0 \; ; \quad \int_0^{2\pi} h(\xi,\theta)d\theta = 0 \tag{5.4}$$

For the compressor itself, we recall the general scaled pressure-rise formula of Eq. (2.7), and the definition of a in Eq. (3.4). For N stages,

$$\frac{p_E - p_1}{\rho U^2} = NF - \frac{1}{2a}\left(2\phi_\xi + \phi_\theta\right) \tag{5.5}$$

Pressure Balance of the Entrance Duct

What is wanted is the overall pressure rise, from inlet to exit, including the pressure difference associated with the circumferential velocity component just ahead of the inlet guide vane. The pressure difference from station 0 to station 1 (where the flow is axial) can be written as:

$$\frac{p_0 - p_1}{\rho U^2} = \frac{1}{2} K_G h^2 \tag{5.6}$$

If the IGV entrance is lossless, the entrance recovery coefficient K_G=1, but if a loss does occur, then K_G<1. The exact value of K_G probably has little effect on the overall results.

In the entrance duct upstream of the IGV, we assume irrotational flow, so that a velocity potential exists which, though unsteady, will satisfy Laplace's equation. Specifically, we define $\tilde{\phi}$ so that

$$\tilde{\phi}_\eta = v/U \; ; \quad \tilde{\phi}_\theta = u/U \tag{5.7}$$

Accordingly, at the IGV entrance (point O on Fig. 2.1),

$$(\tilde{\phi}_\eta)_O = \Phi(\xi) + g(\xi,\theta) \; ; \quad (\tilde{\phi}_\theta)_O = h(\xi,\theta) \tag{5.8}$$

Far upstream, in the reservoir, we take $\tilde{\phi}$ itself to be zero because the flow is at rest.

As a general matter, we must solve Laplace's equation for $\tilde{\phi}$ and then apply Bernouilli's equation to evaluate pressure at the point O. For unsteady flow, with our particular definitions of variables, the result is

$$\frac{p_T - p_O}{\rho U^2} = \frac{1}{2}(\phi^2 + h^2) + (\tilde{\phi}_\xi)_O \tag{5.9}$$

The unsteady contribution, $(\tilde{\phi}_\xi)_O$, is due to unsteadiness in both Φ and g. The complexity of this term is reduced if we consider a straight inlet duct, preceeded by a much shorter potential nozzle, as sketched in Fig. 5.1. In the duct, of dimensionless length ℓ_I, the angle-averaged coefficient $\Phi(\xi)$ will be constant. Therefore, in view of Eqs. (5.7) and (5.8), the velocity potential may be immediately written as

$$\tilde{\phi} = (\eta + \ell_I)\Phi(\xi) + \tilde{\phi}'(\xi,\eta) \tag{5.10}$$

where $\tilde{\phi}'$ is a disturbance velocity potential vanishing at $\eta = -\ell_I$, and giving g and h at point O:

$$(\tilde{\phi}'_\eta)_O = g(\xi,\theta) \; ; \quad (\tilde{\phi}'_\theta)_O = h(\xi,\theta) \tag{5.11}$$

The term needed for Eq. (5.11) is simply

$$(\tilde{\phi}_\xi)_O = \ell_I \frac{d\Phi}{d\xi} + (\tilde{\phi}'_\xi)_O \tag{5.12}$$

Pressure Balance of the Exit Duct

In the exit duct, a complicated rotational flow appears even with axial OGV's when axial flow varies with θ. We will use an approximation, somewhat generalized, developed in [3]. We consider the function P, defined below, to be sufficiently small that it satisfies Laplace's equation.

$$P \equiv \frac{p_s(\xi)-p}{\rho U^2} \; ; \quad \nabla^2 P = 0 \tag{5.13}$$

That is, pressure in the exit duct is assumed to differ only slightly from static pressure at discharge (p_s). Now, the streamwise Euler equation, evaluated at the compressor discharge (point E of Figs. 2.1 or 5.1), gives exactly

$$(P_\eta)_E = (\tilde{\phi}_{\eta\xi})_O = \frac{d\Phi}{d\xi} + (\tilde{\phi}'_{\eta\xi})_O \tag{5.14}$$

Thus, the potential problem for P is the same as the one already mentioned for $-\tilde{\phi}'_\xi$: the minus sign is necessary because, in the exit, η points in the streamwise direction, whereas the reverse is true in the entrance. Choosing a constant to make P = 0 at the duct exit, $\eta = \ell_E$, we find

$$P = (\eta - \ell_E) \frac{d\Phi}{d\xi} - \tilde{\phi}'_\xi \tag{5.15}$$

The foregoing simplified analysis assumes that ℓ_E is not smaller than the distance (conservatively, ℓ_I) at which the entrance flow disturbance potential vanishes. If it were much shorter, presumably the second term of Eq. (5.15) should be omitted. Therefore, just as in [3], we introduce a parameter m in the final result for exit pressure change

$$\frac{p_S - p_E}{\rho U^2} = (P)_E = -\ell_E \frac{d\Phi}{d\xi} - (m-1)(\tilde{\phi}'_\xi)_0 \tag{5.16}$$

where m = 2 would refer to a "long enough" exit duct, and m = 1 would refer to a very short one.

Net Pressure Rise to End of Compressor Exit Duct

Between the upstream reservoir (p_T) and the discharge from the exit duct (p_S) is the zone where circumferential pressure variations may arise. Further downstream are the plenum and throttle, which we assume to contain only axisymmetric disturbances. We can now form the net pressure rise in the zone of possible angular variations by combining Eqs. (5.5), (5.6), (5.9) and (5.16). After introducing Eqs. (5.3) and (5.12), the result may be written

$$\frac{p_S - p_T}{\rho U^2} = (NF - \frac{1}{2}\phi^2) - (\ell_I + \frac{1}{a} + \ell_E)\frac{d\Phi}{d\xi} - m(\tilde{\phi}'_\xi)_0$$
$$- \frac{1}{2a}(2\tilde{\phi}'_{\xi\eta} + \tilde{\phi}'_{\theta\eta})_0 - \frac{1}{2}(1 - K_G)h^2 \tag{5.17}$$

Following [3] we identify the left side, which is the total-to-static pressure rise coefficient, as $\Psi(\xi)$ (which also appears in Sections 3 and 4 above), and the first parenthesis on the right as the quasisteady, axisymmetric compressor characteristic, also familiar from Section 3; we notice

that for steady flow with no disturbance, all other terms on the right vanish, leaving the obvious identity $\Psi = \psi_C$.

$$\Psi(\xi) \equiv \frac{p_S - p_T}{\rho U^2} \tag{5.18}$$

$$\psi_C(\phi) \equiv NF(\phi) - \frac{1}{2}\phi^2 \tag{5.19}$$

The second parenthesis on the right of Eq. (5.17) is the effective flow-passage length through the compressor and its ducts, measured in radii of the compressor wheel. This has been denoted as ℓ_C and thus

$$\ell_C \equiv \ell_I + \frac{1}{a} + \ell_E \tag{5.20}$$

As explained in [3], if the compressor lag τ is considered to be purely inertial, one could write

$$\frac{1}{a} = (2NL_R)\left(\frac{1}{R}\right)\frac{k}{\cos^2\gamma} \tag{5.21}$$

The first factor in parentheses is simply the axial length of the compressor, L_R being the axial length of a row; the factor 1/R puts the distance into wheel radians; k is a factor which could account for interrow spacing; and $\cos^2\gamma$ accounts for the tortuous flow path through the compressor, with γ being the effective stagger angle of the blades. Thus, the effective (inertial) path length for the system is longer than the axial length. The total path length ℓ_C has already been mentioned in Section 4 above.

The last term of Eq. (5.17) will be neglected, in effect assuming that the recovery coefficient K_G at the IGV entrance is 1. Finally,

therefore, we may write Eq. (5.17) in the form

$$\Psi(\xi) = \psi_c(\Phi + (\tilde{\phi}'_\eta)_0) - \ell_c \frac{d\Phi}{d\xi} - m(\tilde{\phi}'_\xi)_0 - \frac{1}{2a}(2\tilde{\phi}'_{\xi\eta} + \tilde{\phi}'_{\theta\eta})_0 \qquad (5.22)$$

In this we have used Eqs. (5.3) and (5.11) to express the argument of ψ_c in terms of $\tilde{\phi}'$:

$$\phi = \Phi + (\tilde{\phi}'_\eta)_0 \qquad (5.23)$$

The next step will be to place Eq. (5.22) in the context of the complete compression system, with plenum and throttle, as sketched in Fig. 5.1. Before doing so, we simplify Eq. (5.22) by introducing a generalization of an approximation familiar from Section 3.

An Approximation of the $dh/d\theta = -g$ Type

The disturbance potential $\tilde{\phi}'$ satisfies Laplace's equation

$$\tilde{\phi}'_{\theta\theta} + \tilde{\phi}'_{\eta\eta} = 0 \qquad (5.24)$$

Its value and normal derivative $\tilde{\phi}'_\eta$ at the compressor entrance are needed, which implies that Eq. (5.24) must be solved as part of our analysis. We would like to avoid the difficulties of such a procedure, if possible.

We know that g is a periodic function of θ, and, by definition, must have a vanishing average over 2π. Therefore, it has a Fourier series and the solution of Eq. (5.24) is

$$\tilde{\phi}' = \sum_{n=1}^{\infty} \frac{1}{n} e^{n\eta}(a_n \sin n\theta + b_n \cos n\theta) \quad ; \quad \eta \leq 0 \qquad (5.25)$$

vanishing at $\eta = -\infty$.

Now, if only the first term of Eq. (5.25) were kept, one would conclude that

$$(\tilde{\phi}'_\eta)_0 = -(\tilde{\phi}'_{\theta\theta})_0 \tag{5.26}$$

which, in view of Eq. (5.11), is precisely the familiar $dh/d\theta = -g$ relation. Thus, it will be expedient to use the value of $\tilde{\phi}'$ at $\eta = 0$ as dependent variable, using the notation Y for simplicity:

$$(\tilde{\phi}')_0 \equiv Y(\xi,\theta) \quad ; \quad (\tilde{\phi}'_\eta)_0 = -Y_{\theta\theta} \tag{5.27}$$

Now Eq. (5.22) takes the form

$$\Psi(\xi) = \psi_c(\Phi - Y_{\theta\theta}) - \ell_c \frac{d\Phi}{d\xi} - mY_\xi + \frac{1}{2a}(2Y_{\xi\theta\theta} + Y_{\theta\theta\theta}) \tag{5.28}$$

Eq. (5.27) implies

$$h = Y_\theta \quad ; \quad g = -Y_{\theta\theta} \tag{5.29}$$

Therefore, if Y is simply required to be periodic in θ, as it obviously must be to describe a physical quantity in the compressor,

$$Y(\xi,\theta+2\pi) = Y(\xi,\theta) \tag{5.30}$$

then the cyclic integrals of g and h vanish,

$$\int_0^{2\pi} g(\xi,\theta)d\theta = 0 \quad ; \quad \int_0^{2\pi} h(\xi,\theta)d\theta = 0 \tag{5.31}$$

as we know they must do; in the case of g by definition, and in the case of h because no circulation can arise in the inlet as we have described the flow there. It is also obvious from the general solution of Eq. (5.25) that the cyclic integral of $\tilde{\phi}'$ itself must vanish, so we know that Y should have the property

$$\int_0^{2\pi} Y(\xi,\theta)d\theta = 0 \tag{5.32}$$

The idea described in Appendix A to improve the accuracy of the $dh/d\theta = -g$ approximation for rotating stall can also be adapted for the present more general case. Corresponding to Eq. (A.6), we write

$$(\tilde{\phi}'_\eta)_0 = -\hat{Y}_{\theta\theta} \quad ; \quad (\tilde{\phi}'_\theta)_0 = \hat{A}\hat{Y}_\theta - \hat{B}\hat{Y}_{\theta\theta\theta} \tag{5.33}$$

Just as in Appendix A, consistency between Eqs. (5.25) and (5.33) can be arranged for two harmonics. Choosing the first two, one finds $\hat{A} = 2/3$ and $\hat{B} = 1/3$, as in Eq. (A.8). Corresponding to Eq. (A.9), one would find the following equation when Eq. (5.33) is used to modify Eq. (5.22)

$$\Psi = \psi_c(\Phi - \hat{Y}_{\theta\theta}) - \ell_c \frac{d\Phi}{d\xi} - m\hat{A}\hat{Y}_\xi + (\frac{1}{a} + m\hat{B})\hat{Y}_{\xi\theta\theta} + \frac{1}{2a}\hat{Y}_{\theta\theta\theta} \tag{5.34}$$

As described in Appendix A, the change is a matter only of coefficients. For present purposes, we will omit this refinement, but keep it in mind for future studies.

Overall Pressure Balance of the Compression System

We now return to Fig. 5.1 and account for pressure changes downstream of the compressor exit, in the plenum and in the throttle. We will derive relations somewhat more general than those already mentioned in Section 4 above.

The plenum will obviously eliminate any spatial variations; thus, it will receive mass at a rate $\rho UA_c\Phi(\xi)$, and discharge mass at a presumably different rate $\rho UA_c\Phi_T(\xi)$. Duct areas at entrance and discharge of the plenum would both presumably be different from the compressor area A_c; the

difference is accounted for in the definition of Φ_T, as in Ref. [5]. If Φ and Φ_T are different, then mass must accumulate in the plenum, changing the density there. As discussed in [5], we can take this change to be isentropic for the situations under consideration.

We assume that the compressor exit discharges as a free jet into the plenum, so that its pressure is $p_S(\xi)$. The isentropic relation between density and pressure then provides that the rate of density change in the plenum is the ratio of dp_S/dt to the square of sound speed, a_S. The rate of increase of stored mass in the plenum volume (V_P) is thus proportional to the dimensionless time derivative of the pressure-rise coefficient $\Psi(\xi)$, defined in Eq. (5.18). The balance of entering, leaving, and stored mass of the plenum can then be written in the following convenient form (see Eq. (4.3)):

$$\ell_c \frac{d\Psi}{d\xi} = \frac{1}{4B^2} [\Phi(\xi) - \Phi_T(\xi)] \tag{5.35}$$

The plenum discharge coefficient Φ_T is of course also the throttle flow coefficient. It must be related to the pressure difference applied to the throttle, and the throttle performance characteristic, in order to complete our overall pressure balance. Generally, these relations would be selected to properly represent an engine application. Here, we consider that the plenum discharges without loss into a throttle duct of length L_T, in which there is a throttle with a pressure-flow coefficient characteristic given by

$$\frac{\Delta p}{\rho U^2} = F_T(\Phi_T) \tag{5.36}$$

The throttle discharges to a reservoir (atmosphere) at the same pressure p_T as that which earlier supplied the entrance to the compressor (see Fig. 2.2). Therefore, the pressure difference $p_S - p_T$ balances the throttle loss and also provides any acceleration of the mass in the throttle duct. In coefficient form,

$$\Psi(\xi) = F_T(\Phi_T) + \ell_T \frac{d\Phi_T}{d\xi} \tag{5.37}$$

In the present paper, we will take the throttle duct as short enough to justify neglecting ℓ_T. This is generally quite a good assumption for realistic throttle ducts. As discussed in Section 3, two typical possibilities for the throttle characteristic, $F_T(\Phi_T)$ are:

$$\text{parabolic:} \qquad \Psi = \frac{1}{2} K_T \Phi_T^2 \tag{5.38}$$

$$\text{linear:} \qquad \Psi = \bar{\Psi} + k_T(\Phi_T - \Phi) \tag{5.39}$$

In any case, having neglected ℓ_T, we write that Φ_T is simply the inversion of F_T:

$$\Phi_T = F_T^{-1}(\Psi) \tag{5.40}$$

In principle, Eqs. (5.35) and (5.40) complete our system of equations for disturbances of the compression system. We imagine that Φ_T may be eliminated between these two equations, and the resulting equation connecting Ψ and Φ can be combined in some way with Eq. (5.28). If so, there are only two equations, so far, for the three unknowns $\Psi(\xi)$, $\Phi(\xi)$, and $Y(\xi,\theta)$. The third equation comes from realizing that Eq. (5.28) involves terms which are functions only of time. If that equation is

integrated over a cycle of θ, the following relation results:

$$\Psi(\xi) + \ell_c \frac{d\Phi}{d\xi} = \frac{1}{2\pi} \int_0^{2\pi} \psi_c(\Phi - Y_{\theta\theta})d\theta \tag{5.41}$$

This integral relation is, in effect, the needed third equation.

Equations of a General Disturbance

For convenience, we assemble the three pressure-balance equations we will use in subsequent analysis, giving them new numbers.

$$\Psi(\xi) + \ell_c \frac{d\Phi}{d\xi} = \psi_c(\Phi - Y_{\theta\theta}) - mY_{\xi} + \frac{1}{2a}(2Y_{\xi\theta\theta} + Y_{\theta\theta\theta}) \tag{5.42}$$

$$\Psi(\xi) + \ell_c \frac{d\Phi}{d\xi} = \frac{1}{2\pi} \int_0^{2\pi} \psi_c(\Phi - Y_{\theta\theta})d\theta \tag{5.43}$$

$$\ell_c \frac{d\Psi}{d\xi} = \frac{1}{4B^2} [\Phi(\xi) - F_T^{-1}(\Psi)] \tag{5.44}$$

where partial differentiation is indicated by subscripts ξ and θ.

Pure Rotating Stall and Pure Surge as Special Cases

It is instructive to see how Eqs. (5.42-5.44) specialize for the pure rotating-stall and surge motions outlined in Sections 3 and 4 above. Surge is the simplest; in that case there is no θ variation, and $Y(\xi,\theta)$ may be set to zero. Eqs. (5.42) and (5.43) are then the same equation, identical to Eq. (4.2). Eq. (5.44) is, of course, identical to Eq. (4.3) for a parabolic throttle line.

For pure rotating stall, the plenum pressure, and the angle-averaged through flow are constant with time; therefore, $d\Psi/d\xi$ and $d\Phi/d\xi$ both are zero. The right side of Eq. (5.44) vanishes, becoming equivalent to a statement that $\Phi = \Phi_T$, and that the operating point must lie on the throttle characteristic (e.g., Eq. (5.38)). Y can be represented as a wave

traveling at speed f; that is, a function of a single variable:

$$Y(\xi,\theta) \equiv Y(\theta^*) \quad ; \quad \theta^* \equiv \theta - f\xi \tag{5.45}$$

The variable θ' is the angle measured in the disturbance frame, and was defined in Section 3. Eqs. (5.42) and (5.43) become, after recalling the definition of λ from Eq. (2.3):

$$\lambda \frac{d^3Y}{d\theta^{*3}} + mf \frac{dY}{d\theta^*} - [\Psi - \psi_c(\Phi - \frac{d^2Y}{d\theta^{*2}})] = 0 \tag{5.46}$$

$$\Psi = \frac{1}{2\pi} \int_0^{2\pi} \psi_c(\Phi - \frac{d^2Y}{d\theta^{*2}}) d\theta^* \tag{5.47}$$

Next, we recall Eq. (5.29) and see that now

$$\frac{dY}{d\theta^*} = h \quad ; \quad \frac{d^2Y}{d\theta^{*2}} = -g \tag{5.48}$$

This last equation converts Eq. (5.46) precisely to the governing equation of pure rotating stall, Eq. (3.2). Eq. (5.47) is converted to

$$\Psi = \frac{1}{2\pi} \int_0^{2\pi} \psi_c(\Phi + g) d\theta^* \tag{5.49}$$

which the definitions of δ and G in Section 3 show to be identical to Eq. (3.12) for performance effect of rotating stall. Thus, the reduction of our general disturbance equations to pure rotating stall is demonstrated.

Application of One-Term Galerkin Procedure

To treat a general disturbance which may have both angular variation like rotating stall and time-dependent mean flow like surge will require solution of the complete system of Eqs. (5.42-5.44), which is third order in angle, but only first order in time. This circumference suggests that

a Galerkin treatment of angle dependence would be helpful to eliminate the angle dependence and reduce the system to three ordinary differential equations, with time as the only independent variable.

Section 3 above indicates how to proceed with the Galerkin procedure. We have two issues to settle before beginning, however. First, should we imitate Section 3 closely by working in a traveling frame (θ^*), or should we stay in the "laboratory frame" (θ)? Study shows there is no advantage and many conceptual difficulties in the former system, while the latter is perfectly general, depending only on the obvious consideration that physical quantities must be periodic in wheel angle whether or not a permanent wave is in progress; therefore, we will apply the Galerkin procedure in laboratory coordinates.

Second, shall we be satisfied with the one-term harmonic representation of angular variation? For the present study, there seems no good alternative if we want to keep a relatively simple form. Even if we found a better functional form to represent the rotating-stall profiles of Figs. 3.4a-f, it is not clear that that would be helpful for general disturbances, some of which might be weak transients which actually would be well represented by a simple harmonic wave. Although we might consider extending the analysis to higher harmonics, experience with a two-harmonic approach (for pure rotating stall) suggests that such an extension would have to be carried to high harmonic order to be valid. For the present, we will accept the accuracy limitations inherent in a one-harmonic model.

Recalling Eq. (3.17), we represent Y as follows:

$$Y = WA(\xi) \sin(\theta - r(\xi)) \tag{5.50}$$

We include phase angle $r(\xi)$ in this equation, because we must not expect nodes of the disturbance always to remain in the same angular location. We substitute Eq. (5.50) into Eq. (5.42), and find that the residual (analogous to Eq. (3.18)), moments of which will be made to vanish, is

$$\frac{1}{W} L = -\frac{1}{W}\left[\Psi + \ell_c \frac{d\Phi}{d\xi} - \psi_c(\Phi + WA \sin(\theta-r))\right] - (m+\frac{1}{a}) \frac{dA}{d\xi} \sin(\theta-r)$$
$$+ [(m+\frac{1}{a}) \frac{dr}{d\xi} - \frac{1}{2a}]A \cos(\theta-r) \qquad (5.51)$$

where Ψ, Φ, A, and r are to be functions of ξ alone.

We now set the moments of Eq. (5.51) equal to 0. The integral of L must vanish; this accounts directly for one of the basic equations, Eq. (5.42):

$$\frac{1}{2\pi} \int_0^{2\pi} \psi_c(\Phi + WA \sin\zeta)d\zeta = \Psi + \ell_c \frac{d\Phi}{d\xi} \qquad (5.52)$$

The $\sin(\theta-r)$ moment is

$$\frac{1}{\pi W} \int_0^{2\pi} \sin\zeta \ \psi_c(\Phi + WA \sin\zeta)d\zeta = (m + \frac{1}{a}) \frac{dA}{d\xi} \qquad (5.53)$$

and the $\cos(\theta-r)$ moment is

$$\frac{1}{\pi W} \int_0^{2\pi} \cos\zeta \ \psi_c(\Phi + WA \sin\zeta)d\zeta = -[(m + \frac{1}{a}) \frac{dr}{d\xi} - \frac{1}{2a}]A \qquad (5.54)$$

Without yet specifying the characteristic function ψ_c, we see that if it is a regular function of ϕ, the integral on the left must vanish when carried out over a complete cycle. Thus, very generally, it is clear that $dr/d\xi$ must be a constant if A is not to be zero. Calling that constant f_o,

$$r = f_o \cdot \xi \quad ; \quad f_o \equiv \frac{1/2}{1 + ma} \tag{5.55}$$

Actually, f_o is the propagation speed found in [3] for small-disturbance rotating stall (which is a simple harmonic wave). We conclude that, even though the amplitude A varies with time within the context of the one-term approximation, nodes of the wave of angle dependence must travel at a constant speed comparable to that of pure rotating stall.

We are left with Eqs. (5.44), (5.52), and (5.53) to determine the unknown functions of time, Ψ, Φ, and A.

Final Simplified Equations

It remains to specify the axisymmetric characteristic; we adopt the cubic function defined in Eq. (3.21), making the substitution

$$\frac{\phi}{W} - 1 = \frac{\Phi}{W} - 1 + A \sin\zeta \tag{5.56}$$

It is obvious that if ψ_C can be expressed as a sum of powers of ϕ, only even powers of A $\sin\zeta$ will contribute to the integral in Eq. (5.52), and only odd powers in Eq. (5.53). Inspection of those equations then shows that A will enter as the square, no matter what the particular form of ψ_C. For convenience, we define a new variable J to replace A:

$$J(\xi) \equiv A^2(\xi) \tag{5.57}$$

and we note that J must always be positive. Carrying out the indicated integrals, we find the governing equations to be

$$\frac{d\Psi}{d\xi} = \frac{W/H}{4B^2}\left[\frac{\Phi}{W} - \frac{1}{W}F_T^{-1}(\Psi)\right]\frac{H}{\ell_c} \tag{5.58}$$

$$\frac{d\Phi}{d\xi} = \left[-\frac{\Psi-\psi_{co}}{H} + 1 + \frac{3}{2}\left(\frac{\Phi}{W} - 1\right)\left(1 - \frac{1}{2}J\right) - \frac{1}{2}\left(\frac{\Phi}{W} - 1\right)^3\right]\frac{H}{\ell_c} \tag{5.59}$$

$$\frac{dJ}{d\xi} = J\left[1 - \left(\frac{\Phi}{W} - 1\right)^2 - \frac{1}{4}J\right]\frac{3a\ H}{(1+ma)W} \tag{5.60}$$

These are our final equations for instantaneous values of flow coefficient (Φ), total-to-static pressure rise (Ψ), and squared amplitude of angular variation (J), all as functions of time (ξ).

6. DISCUSSION OF SIMPLIFIED EQUATIONS

Pure Modes and Their Growth

Our intention is to use the foregoing Eqs. (5.58-5.60) to compute the consequences of an initial disturbance of a compression system. Before doing that, we should examine these equations to discover what we can about their general features.

First, we observe how these equations describe pure surge or rotating stall. In the case of pure surge, $J = 0$, and Eq. (5.59) becomes simply Eq. (4.2) with cubic ψ_c (Eq. (3.13)). Eq. (5.58) is the familiar Eq. (4.3), in effect. In pure rotating stall, amplitude J is constant, and the bracket on the right of Eq. (5.60) must vanish, establishing an "equilibrium" J_e:

$$J_e = 4[1 - (\frac{\Phi}{W} - 1)^2] \tag{6.1}$$

In this case, Φ will also be constant because there is no surge, and we can identify $(\Phi/W) - 1$ as the quantity β introduced in Section 3 to describe average flow coefficient, and show that J_e is simply the A^{*2} for pure rotating stall in Eq. (3.20). We may also observe that when this value of J is inserted into Eq. (5.59), and $d\Phi/d\xi$ is set equal to zero, that equation reduces to the one-harmonic Galerkin solution for performance effect (δ) in rotating stall, presented in Eq. (3.22).

Our equations appear to permit the existence of pure modes; that is, either surge or rotating stall without the other. However, we should question whether such modes could evolve from initially infinitesmal disturbances. Clearly, such a process is possible for pure surge; if J is

zero it will remain zero, according to Eq. (5.60), and the other two equations will deal with the evolution of pure surge disturbances, as described in Refs. [5] and [6].

It appears to be impossible, however, for rotating stall to evolve without producing at least some disturbance of Φ or Ψ; if J changes, then Eq. (5.59) says that Ψ or Φ must also change. A disturbance of Φ induced in this way might of course be a non-cyclic transient, not to be identified as "surge". Small values of B are associated with rotating stall in preference to surge (Ref. [5]). The present Eqs. (5.58), (5.59) suggest that if B is small enough, and the throttle is steep enough, Φ could remain essentially constant while J grows. The solution of Eq. (5.63) in that case is

$$\frac{J}{J_e} = \frac{1}{1 + \left(\frac{J_e}{J_o} - 1\right) \exp\left[-\frac{3aJ_e H/W}{4(1+ma)}\,\xi\right]}$$

where J_o is an assumed initial disturbance. The essence of the solution is that J grows steadily from J_o to its final, fully-developed pure rotating-stall value of J_e.

Figure 6.1 shows this behavior for the compressor geometry discussed in Section 4. For reference the relevant parameters are: m = 1.75, H = 0.18, W = 0.25, 1/a = 3.5. The calculations have been done for three different values of J_e/J_o: 10^{+2}, 10^{+4}, and 10^{+6}. If we consider the transient to occur at Φ = 0.25 (i.e., β=0), then this implies initial rotating stall amplitudes of 0.2, 0.02, and 0.002, respectively.

The graph shows the normalized rotating stall amplitude A/A_e (= $\sqrt{J/J_e}$

versus time, with time being plotted in rotor revolutions (1 rev = $2\pi\xi$). It is clear from the figure that the growth is dependent on the initial conditions. This can be seen from Eq. (6.2) which, if $J_o << J_e$, for small times can be written as

$$J - J_o = J_o \left(\frac{3aJ_e H/W}{4a(1+ma)}\right)\xi + \ldots$$

i.e., the increment of J is proportional to the initial value. Once the value of J has grown so that the nonlinear aspects of the process become important, however, the growth rate to the final limit cycle amplitude becomes independent of the initial conditions. This can be seen by noting that if the curves for $J_e/J_o = 10^2$ and 10^6 were translated (in time) such that they matched with the curve for $J = 10^4$ at the point where $J/J_e = 0.2$, say, the three curves would be virtually identical all later times. This type of behavior, which is typical of nonlinear systems, will also be encountered later, when we discuss the results for the combined rotating stall/surge transients.

Eq. (6.2) says that, for any given value of β, the time needed to approach J within a closeness defined by

$$\frac{J_e - J}{J_e} = \frac{1}{e} \tag{6.3}$$

is

$$\xi_e = \frac{1+ma}{3a(1-\beta^2/W^2)H/W} \ln \frac{J_e}{J_o} \tag{6.4}$$

Thus, if $J_o << J_e$, the time of final approach is proportional to $\ln J_o$.

Also, the time for rotating-stall development is short for steep diagrams (large H/W), and for throttle settings just inside the stall zone (β less than but close to 1). The fastest approach would occur if the compressor were already (transiently) in the middle of the steady-state rotating stall zone ($\beta = 0$) before rotating stall first appeared.

Nature of the Coupling Process

We have seen that Eq. (5.60) describes how angular-disturbance amplitude J grows at a rate which initially depends only on the disturbance itself, but then, in the manner of a chemical reaction, tries to approach an equilibrium described by Eq. (6.1). In general, the flow coefficient will change with time, so that during a coupled oscillation, $J_e(\xi)$ will be a moving target, so to speak, for J. Whether J actually achieves and stays on that target, that is, quasisteady equilibrium with $\Phi(\xi)$, will be known only from simultaneous solution of the equations, giving in effect a trajectory in the three-dimensional space Ψ, Φ, J.

Inspection of Eq. (5.60) also shows that excursions of Φ away from the central point $\Phi = W$ will diminish the rate of change of J. Thus, if we suppose a throttle setting of $\Phi = W$ (i.e., $\beta = 0$), then the presence of surge-like variations of Φ will tend to suppress circumferential variations. Thus, if B is small, Eq. (5.58) implies that swings of Φ will tend to be small, which, relatively, would encourage circumferential variation, according to Eq. (5.60).

Turning to Eq. (5.59), we see that the presence of a circumferential angular variation in velocity will diminish the term in which J appears (recalling that J must always be positive). That term describes the

central slope of the characteristic, at the midpoint of Fig. 3.2, thus reducing the basic amplifying effect of the characteristic in the stall region. We can conclude that this variation (i.e., the presence of a rotating stall-like disturbance) would tend to inhibit surge-like disturbances of Φ.

The foregoing arguments, which are certainly in qualitative agreement with the many experimental observations that have been made of these phenomena, only suggest how "surge-like" and "rotating stall-like" disturbances are coupled through Eqs. (5.59), (5.60). The coupling is mediated by Eq. (5.58), and one must carry out trajectory calculations to see the actual consequences of a given initial disturbance.

Small Surge Disturbance of Rotating Stall

We know that our equations permit both pure surge and pure rotating stall. We might go further and ask whether those "pure" motions are stable to disturbances of the other family. First, we imagine a case of fully-developed rotating stall subject to weak surge-like disturbance. Assuming an infinitely steep throttle line ($k_T = \infty$ in Eq. (4.4)), and eliminating Ψ between Eqs. (5.58, 5.59) by differentiation, while holding J constant, one finds a harmonic-oscillator equation for $\Phi(\xi)$, with the damping term

$$\text{damping:} \quad -\frac{3}{2}\left[1 - \frac{1}{2}J - \frac{\beta^2}{W^2}\right]\frac{1}{W}\frac{d\Phi}{d\xi} \tag{6.5}$$

Damping would be negative, if J were zero. However, if J is fully developed, then J is actually $4(1 - \beta^2/W^2)$, which makes Eq. (6.5) positive:

$$\text{damping:} \quad + \frac{3}{2}\left[1 - \frac{\beta^2}{W^2}\right] \frac{1}{W} \frac{d\Phi}{d\xi}$$

and we conclude that small-disturbance surge-type oscillations tend to have positive damping in the presence of "equilibrium" rotating stall. Therefore, any surge-like disturbance of pure rotating stall would therefore decay, which might be inferred from the fact that the relevant compressor curve is now the negatively-sloped fully developed rotating-stall curve. A careful stability analysis of Eqs. (5.58-5.60) should be carried out; quite possibly the matter is more complex than the foregoing argument implies.

Small Angular Disturbance of Surge

Next, we suppose that an equilibrium surge oscillation is in progress, and ask what happens when a small rotating-stall-like disturbance (J_o) is introduced. Eq. (5.60) will govern the growth or decay of J. We note that Φ will vary during the surge oscillation so that the bracket of Eq. (5.60) may be either positive or negative, and it is therefore not obvious whether, on balance, J will grow or not.

To estimate the effect of Φ, we recall the pure surge equation, Eq. (4.6), and set $k_T = \infty$ (steep throttle line). Then, the surge equation takes the same form as Eq. (3.9) for rotating stall, with the time variable $\xi/(2B\ell_c)$ playing the role of θ^*. We can therefore adapt the Galerkin solution for rotating stall (Eq. (3.21)) to represent surge:

$$\Phi - \bar{\Phi} = 2W\sqrt{1 - \beta^2/W^2}\,\sin\left(\frac{\xi}{2B\ell_c}\right) \tag{6.6}$$

Identifying $(\bar{\Phi}/W) - 1$ as β/W and introducing Eq. (6.6) into Eq. (5.60)

gives, after simplification,

$$\frac{1}{J}\frac{dJ}{d\xi} = \frac{3aH/W}{1+ma}\left[-\left(1-\frac{\beta^2}{W^2}\right) - 4\frac{\beta}{W}\sqrt{1-\frac{\beta^2}{W^2}}\sin\frac{\xi}{2B\ell_c}\right.$$

$$\left. + 2\left(1-\frac{\beta^2}{W^2}\right)\cos 2\frac{\xi}{2B\ell_c} - \frac{1}{4}J\right] \qquad (6.7)$$

If we then neglect J within the bracket on the ground of small disturbances, the foregoing equation can be integrated to give the level of J predicted to exist at any time ξ during the disturbance:

$$\frac{J}{J_o} = \exp\left\{\frac{3aH/W}{1+ma}2B\ell_c\left[-\left(1-\frac{\beta^2}{W^2}\right)\frac{\xi-\xi_A}{2B\ell_c} + 4\frac{\beta}{W}\sqrt{1-\frac{\beta^2}{W^2}}\cos\frac{\xi}{2B\ell_c}\right.\right.$$

$$\left.\left. + \left(1-\frac{\beta^2}{W^2}\right)\sin 2\frac{\xi}{2B\ell_c}\right]\right\} \qquad (6.8)$$

where a constant of integration ξ_A is included. The question is, whether J is greater or less than its initial value J_o.

If the curly bracket of Eq. (6.8) is positive, $J>J_o$, while, if it is negative, $J<J_o$. Examining that expression in detail, one sees that the first term in the square bracket, being negative and increasing, represents a tendency for J to be progressively smaller than J_o for large time. The oscillatory harmonic terms could reverse that tendency for early or moderate times.

Fig. 6.2 illustrates the possibilities for the special case of $\beta = 0$. The square bracket, the sign of which indicates whether J is greater or less than its initial value J_o, takes the form

$$\text{growth factor:} \quad \left[-\frac{\xi - \xi_A}{2B\ell_c} + \sin 2 \frac{\xi}{2B\ell_c} \right] \tag{6.9}$$

The first and second terms of this expression are plotted separately on Fig. 6.2. A series of lines are shown to represent the first term, because ξ_A is arbitrary. Where any one of these lines cross the sine wave is a possible starting time for the disturbance. What happens after the starting time clearly depends on the phase of the sine wave (surge) when the angular variation starts. If the start is at $\xi = 0$, then the shaded area above line (1) shows the duration and intensity of the excursion of J. The duration is less than a quarter period of the surge oscillation. Whether the amplification rate is sufficient during this period for rotating stall to develop cannot be found from this small-perturbation solution.

If the intersection point is moved along the sine wave, the time available for amplification shortens, until line (2) is reached for which there can be no growth at all. Not until line (3) is reached does amplification again become positive. The greatest tendency for rotating stall to grow is found for line (4).

In order better to visualize these results, we sketch on Fig. 6.3 the cubic compressor characteristic, and overlay a surge cycle sketched as a counterclockwise circle centered at $\beta = 0$. We indicate by dark lines on the circle certain phase zones. If an angular disturbance initiates in one of those zones it will, at least briefly, amplify. Outside those zones, amplification of a weak angular disturbance cannot occur. Points are labeled on Fig. 6.3 to show correspondence with the lines of Fig. 5.1.

The foregoing discussion indicates that it is very important to know the precise character of an initial disturbance, and the timing of its introduction, whether it is velocity-like or pressure-like, and its magnitude. All those factors could have a profound effect on the ultimate trajectory of the disturbance.

Summary of Qualitative System Behavior

Before showing the numerical results for the trajectories in Φ, Ψ, A space, we can summarize the conclusions that we have drawn so far about the system behavior:

(1) Pure modes of either surge or rotating stall are permitted as permanent oscillations.

(2) Pure surge can evolve from an initial weak axisymmetric disturbance.

(3) In principle, pure rotating stall cannot evolve directly from a weak angular disturbance; some axisymmetric disturbance will be induced. Small B-parameter and steep throttle characteristic would favor growth into pure rotating stall.

(4) The growth rate of an angular disturbance (towards a limit cycle value) depends initially on the strength of the initial disturbance, but becomes independent of this when the nonlinear aspects of the process become important.

(5) Angular disturbances will grow toward an equilibrium value depending on the instantaneous flow coefficient; if the latter is also changing with time, angular-disturbance amplitude "chases a moving target".

(6) Excursions of flow coefficient will tend to suppress angular variations, and the presence of angular variations will tend to

suppress surge.

(7) Any small surge-like disturbance in the presence of fully-developed rotating stall will tend to decay.

(8) In the presence of fully-developed surge, a small angular disturbance may decay or may grow (but only during a fraction of one surge cycle), depending on the phase of the surge cycle in which the disturbance originates.

7. NUMERICAL RESULTS FOR GENERAL POST-STALL TRANSIENTS

The set of coupled ordinary differential equations given as Eqs. (5.58), (5.59), and (5.60) have been solved numerically for a representative set of parameters to show some of the basic features of the phenomena. Specifically, calculations have been carried out to illustrate the effects of the non-dimensional parameters B and ℓ_c as well as of the initial conditions. In view of the approximate nature of the approach taken, it is to be emphasized, however, that no extensive parametric study has been performed.

In the calculations, the axisymmetric compressor characteristic has been taken to be the same cubic curve that was described in Section 3, and this is shown for reference as the solid line in Fig. 7.1. Except as noted otherwise, the throttle line used is the parabola that is shown as the dash-dot line in this figure. As mentioned in Section 3, these curves are representative of a three-stage, low-speed compressor, such as that used in Ref. [5].

Unless specified, the initial values of non-dimensional pressure rise and flow coefficient are taken to be the values at the peak of the curve, i.e., $\Phi = 0.5$ and $\Psi = 0.66$. At that condition, we shall imagine that a certain level of circumferential nonuniformity defined by A(0) appears at time $\xi=0^*$. The system of equations (5.58-5.60) governs the ensuing transient which, owing to coupling, may show either temporal (surge-like) or circumferential (rotating-stall-like) variations.

---

*Recall that the nondimensional amplitude of the θ-dependent velocity nonuniformity is AW, and $A \equiv \sqrt{J}$.

Effect of B Parameter

We start by demonstrating how our equations give a more or less familiar effect, that of the B parameter. (This has previously been well documented [5,6] as far as the overall system response is concerned.) Figure 7.2 shows the transient system response in terms of the overall pressure rise (atmosphere to plenum) and annulus averaged flow coefficient for three different values of B; 1.0, 1.4, and 2.0. Also indicated in Fig. 7.2 is the axisymmetric curve (the solid line) and the calculated rotating stall curve, which is shown dashed. In these calculations, the value of ℓ_c was 8.0 and the initial rotating stall amplitude A(0) was one percent of the average velocity, i.e., the initial non-dimensional amplitude of velocity perturbation was 0.005.

It is seen that the higher values of B cause greater excursions in axial velocity. At the highest value, this would lead to surge cycles. For the lower values, the eventual result of the initial transient is operation at a new equilibrium point on the rotating stall curve.

As mentioned, the picture shown in Fig. 7.2 is a somewhat familiar one, but is nevertheless remarkable in that it follows from the present general transient equations. Figure 7.3 presents a new, more detailed view of these same transients. This latter figure shows the rotating stall amplitude, $A(\xi)W$ $(= \sqrt{JW})$, versus annulus-averaged flow coefficient (Φ) for the same three values of B, and the same value of ℓ_c and initial conditions. Also indicated in the figure is the locus of steady-state rotating-stall amplitudes for different values of Φ; in other words, the amplitude one would have in steady-state operation at that

particular mass flow. This is just the value of amplitude that would be predicted from Eq. (3.21). For the cubic characteristic used, the steady-state amplitude has a maximum at $\Phi = 0.25$ and goes to zero (i.e., steady-state rotating stall ceases) at $\Phi = 0.5$ and $\Phi = 0.0$. This curve of amplitude gives the "equilibrium" toward which rotating-stall-like disturbances must tend.

An obvious feature of these transients is that over the first part, for Φ greater than roughly 0.25, the amplitude during the transient is substantially less than that during steady-state operation. However, for lower flows than this, the amplitude can actually exceed the steady-state value. In addition, as seen in the curve for $B = 2.0$, the rotating stall persists into the reverse-flow regime during the transient. This can be contrasted with steady-state operation in which, for this compressor, rotating stall cannot exist when flow is reversed.

It should be noted that when the transient is of the surge type, calculations have only been carried out for part of the initial cycle. The reason for this is that the stall-cell amplitude decays to a very low value during the extended operation at reverse flow. Thus the "initial condition" for the part of the transient when the flow through the compressor accelerates from zero back to unstalled operation is essentially that of zero stall-cell amplitude. Under these conditions, as discussed in Section 6, there will be no subsequent growth of rotating stall, and the transient will proceed as pure surge.

It does not seem physically realistic, however, that there would be a lower level of flow asymmetry during a surge cycle than during operation

prior to stall, and thus this part of the calculation does not appear to be a valid description. It might be more correct to say that there is always some minimum disturbance amplitude present, able to provide an "initial disturbance" at any time. Although there is certainly no bar to including this in the numerical integration routine, in view of the lack of information about this point, we have not elected to do this, but rather to restrict computations to the first part of each transient. We will return to a discussion of this point in the next section.

The basic feature shown in these calculations is the growth and decay of the rotating stall, either to zero or to the appropriate "stagnation" value, as the mass flow varies. That this process must occur has been known qualitatively for some time. As far as the authors know, however, this is the first time that it has been calculated, in even an approximate manner, using the equations of motion for asymmetric flow in a compressor.

Effect of Initial Conditions

In addition to the B parameter, the effect of the initial level of disturbance A(0)W was also examined. Results are shown in Fig. 7.4, which shows the locus of the compressor operating point in the AW, Φ (rotating stall amplitude/flow coefficient) plane. The calculations shown are for B = 1.0, ℓ_c = 8.0, and for three different initial values of rotating-stall amplitude: 0.05, 0.005, 0.0005. These correspond respectively to initial velocity perturbations of ten percent, one percent, and one-tenth percent of the mean axial velocity. It can be noted that the last of these is roughly the size that would be expected in a good wind tunnel test section and the first appears to be larger than the long-wavelength velocity

disturbances that are seen prior to rotating stall. Thus, our range of initial disturbance amplitude conditions encompasses essentially all physically plausible situations. The value that we regard as our "base case", the one percent level, might be a reasonable estimate for the magnitude of velocity non-uniformities to be expected prior to rotating stall, but there seems to be little data on this point.

In Fig. 7.4, the locus of steady-state rotating stall amplitude is again indicated by the crosses. The eventual equilibrium point in rotating stall, at $\Phi = 0.35$, $\Psi = 0.455$, is also indicated as point E.

The effect of the initial condition is strongly evident early in the transient, since the growth rate is proportional to the amplitude of the perturbation. After the stall amplitude has reached a certain size, however, on the order of 0.1-0.2, the nonlinear effects become important, and the slope of the trajectory does not depend strongly on the initial conditions. Although there are some differences in the extent of the excursion in axial velocity between the three cases, the behavior once the trajectory approaches the vicinity of the steady-state locus is fairly similar for the three cases. As discussed in Section 6, this relative independence from the initial conditions during the approach to the equilibrium state is typical of nonlinear systems of the type which we are examining.

The effect of the initial condition can also be shown in a Φ, Ψ representation, as in Fig. 7.5. Here, only the curves for initial amplitudes 0.05 and 0.0005 are shown. It can be seen that even though there are two orders of magnitude of difference between the initial

amplitudes, the trajectories of the plenum pressure versus flow coefficient are not at all dissimilar; they both show roughly the same excursion in mass flow before ending up at the eventual equilibrium point in rotating stall, denoted on the graph by E.

We can also look more directly at the influence of initial conditions on the compressor pumping characteristic, i.e., the compressor output. This is found by subtracting the momentum changes in the compressor duct from the overall (atmosphere to plenum) pressure rise. The compressor pumping characteristic is given by

$$\text{Nondimensional pressure rise} = \psi_c(\Phi) + \delta \tag{7.1}$$

where now δ is a function of time. The result of doing this is seen in Fig. 7.6. This figure presents the instantaneous compressor pressure rise versus the instantaneous annulus-averaged axial velocity parameter, for the same conditions as in Fig. 7.5, namely B = 1.0, ℓ_c = 8.0, and initial amplitudes A(0) = 0.05 and 0.0005.

The trajectory for 0.0005 can be seen to follow the axisymmetric characteristic until near $\Phi \sim 0.25$ (the point of maximum steady-state rotating stall amplitude), and then depart from that curve and thereafter follow the steady-state rotating-stall curve quite closely. The trajectory for 0.05 departs from the axisymmetric curve virtually from its initial point (showing the influence of nonlinearity) and tracks essentially along the steady-state rotating-stall curve once it has passed through ψ_c for the first time. The eventual equilibrium point is again indicated in the figure as E.

Calculations have also been carried out for other values of B to examine the effect of initial conditions. These confirm, in general, the trends shown in the preceeding figures, namely that over a fairly wide range of initial conditions, the results do not depend strongly on the precise values used. There are, however, situations in which the initial condition can make a great deal of difference in the eventual outcome. For example, if one is on the "borderline" with regard to encountering eventual surge or rotating stall, then a change in the initial amplitude can alter the system behavior, from tending to a new equilibrium point to undergoing a surge cycle. The range of situations in which the initial condition had a significant effect on the ultimate result was not investigated in any detail. From the few studies that have been carried out, it appears that if B differs by more than about 10 percent from the transition value, then the influence of the initial condition is substantially diminished. It is felt, however, that the possible influence of initial conditions, and thus the question of how to specify initial conditions properly, (as well as the details of the nature of disturbances at different stages of the surge cycle), is one that must be investigated further.

It is also to be noted that one can always produce changes in system behavior by making sufficient changes of initial conditions. For example, if one decreases the initial amplitude to 0.00005 (0.01% of mean velocity), the growth of the rotating-stall cell will be so slow during the transient that the compressor behavior will be virtually on the axisymmetric curve throughout, and a surge will finally result. As

discussed previously, however, it is felt that this represents an unrealistically weak initial disturbance. We therefore feel somewhat encouraged that the calculations will not be very sensitive to the initial conditions, although the matter clearly deserves more study.

Effect of Compressor Length to Radius Ratio

The other parameter investigated was ℓ_c, the compressor length-to-radius ratio. Results are shown in Fig. 7.7, in which trajectories for values of ℓ_c of 4.0, 6.0, and 8.0 (the base case) are shown. The value of B is 1.0 and the initial condition is kept at A(0) = 0.005. As in previous figures, the steady-state value of rotating stall amplitude and the equilibrium value are also indicated.

It can be seen that the curves for ℓ_c = 8.0 and 6.0, while quantitatively different, have the same qualitative features, namely a rapid rise in amplitude and then an essentially quasi-steady tracking along the steady-state amplitude curve until the equilibrium value is reached. A completely different situation exists for ℓ_c = 4.0, however. There is a large discrepancy between the calculated unsteady trajectory and the steady-state curve and in fact, the system does not settle down to a new equilibrium point. Starting from the initial conditions, the mass flow decreases then increases again and the stall cell amplitude decays to a negligible value. In other words, the compressor goes into rotating stall and then comes out again, returning to the unstalled portion of the compressor characteristic. This behavior would thus be a kind of surge excursion, rather than an approach to a new system equilibrium in rotating stall.

These calculations show that, in addition to the B parameter, the length to diameter ratio, ℓ_c, also can affect whether a given system will exhibit surge or rotating stall. The reason is that, for the same value of B, a decrease in length-to-radius ratio means that the time for the formation of a rotating stall cell is relatively longer in proportion to the time for a mass flow excursion. This idea appeared in the discussion in Section 1 concerning the ratios of different times; it was pointed out that the ratio of both the Helmholtz resonator time and the flow-change time to the rotating-stall formation time will scale with length-to-radius ratio.

It is relevant here to briefly relate these calculations to previous studies. In [5] the only effect that was investigated was the influence of the B parameter. In the published results, the "time constant" that characterized the rotating-stall formation time was kept constant at two rotor revolutions, since the available data was insufficient to determine it more precisely. It was, however, stated that some calculations had been carried out using different values of that time constant and the results for the critical value of B were somewhat different, although over the range examined the difference was not great. In the present study, there is no need to assume such a time constant, because we are now actually calculating the manner in which the compressor output transitions from axisymmetric to fully developed rotating stall.

Comparison with Data on Instantaneous Compressor Performance

In addition to examining the impacts of B parameter, initial conditions, and compressor length-to-radius ratio, we have also used the

present calculation procedure to help in the interpretation of some transient compressor data. The situation is as follows: We have taken data from a surge cycle, in the form of overall atmospheric to plenum pressure rise versus mass flow, and from this we have attempted to estimate the instantaneous compressor pumping characteristic.

The specific procedure we have followed is to subtract from this overall pressure rise a one-dimensional (i.e., axisymmetric) correction for the inertial forces due to fluid accelerations during the surge cycle. The explicit expression for the correction is:

$$\psi_c = \Psi + \ell_c \frac{d\Phi}{d\xi} \tag{7.2}$$

Note that this is only valid for axisymmetric flow. The terms given by the data are Ψ and $\ell_c \, d\Phi/d\xi$, and ψ_c is calculated. The details of this procedure are given in [7,8].

In applying this procedure to the data, however, it is also necessary to examine the time-resolved data to determine whether the surge includes only axisymmetric flow. It was found that the data showed rotating stall, not fully developed, toward the end of each period of rapid flow change. Although the data are not sufficient to resolve all the details of the flow, one must conclude that axisymmetric flow cannot be assumed for the entire surge transient that the data represents.

A sample of the data is shown in Fig. 7.8, with the inertially corrected characteristics determined by Eq. (7.2). Curves 1 and 2 are found from correcting the accelerating and decelerating portions of the surge cycle, respectively. Also shown in the figure, by the dot-dash line, is the

measured steady-state data for both unstalled and rotating stall operation. It can be seen that even though there is some scatter in the calculated ψ_c, due presumably to the differentiation of the experimental data, the points fall into two categories: For decelerations, the corrected curve lies substantially above the steady-state rotating-stall curve, whereas for accelerations (at least for $\Phi > 0.4$), the derived pumping characteristic is considerably below the steady-state curve. In view of this behavior, the question arises whether a single-valued axisymmetric curve is indeed a valid representation, or whether a more comlex axisymmetric behavior must be invoked.

To try to understand the situation in more detail, calculations have been carried out using the parameters that characterize the transient data. These are B = 1.58, ℓ_c = 8.0, and a throttle setting that corresponds to a throttle curve of K_T = 10. The calculations were done both for accelerating and decelerating flows. For the decelerations, the initial conditions were: Φ = 0.5, Ψ = 0.66, and A(0)W = 0.005. For the accelerating part of the cycle the initial conditions were Φ = 0.0, Ψ = 0.3, and A(0)W = 0.005.

The results are shown in Fig. 7.9. The estimated axisymmetric characteristic is the solid line and the steady-state rotating stall curve is the dashed line. The computed instantaneous compressor performance (which corresponds to the quantity shown dashed in Fig. 7.8), is indicated by the heavy dash-dot lines. The arrows show the direction of the motion of the operating point.

It can be seen that the computed and the experimental curves have strong similarities, at least qualitatively. In particular, the tendency

for the compressor pumping characteristic to be above the axisymmetric performance in the reverse flow region and below it at high forward flows is clearly manifested.

The reason for this is found from consideration of the growth and decay of the rotating stall. During the latter part of the deceleration, the instantaneous rotating stall amplitude is much larger than the steady-state value (which is in fact zero for negative values of Φ). Thus the compressor output is closer to that which is characterized by these large values of A. Conversely, during the accelerations, for the flows greater than $\Phi = 0.4$, say, the rotating stall amplitude is again much larger than that in steady-state operation, and the performance (i.e., pressure rise) also corresponds to that associated with large values of stall cell amplitude.

The main points in the foregoing comparison of experimental data with the present computations are thus:

1) The behaviors of the two are qualitatively similar, and
2) The departure of the compressor pumping characteristic from both axisymmetric and steady-state performance is due to the fact that the rotating stall amplitude differs considerably from the steady-state value. In particular, in the latter part of both deceleration and acceleration processes, the stall cell is much "bigger" than one would presume from steady-state considerations, and the performance thus departs considerably from that of the steady-state.

8. DISCUSSION OF THE PRESENT MODEL AND SUGGESTIONS FOR FUTURE WORK

Although the numerical calculations and the analysis have pointed out certain features of the problem which appear to be important, it is clear that the present treatment has only made a start on this very complex problem. It is thus appropriate to give some discussion about those aspects of the actual flow that are included in the theory, those aspects that are potentially important but have not been included, as well as some of the areas that have been pointed up as needing further investigation.

We can start by listing those aspects of the unsteady compressor and compression system behavior that are accounted for:

1) System dynamic characteristics are included. They are analyzed in a lumped parameter fashion. For the situations considered in the present report (low Mach number and low frequency) this is a very good approximation. As either frequency or Mach number is increased, one may have to adopt a more complex description of these components. In particular, there is, for high pressure ratio compressors, the possibility of mass storage within the compressor itself so that a simple representation of the inertance of the flow in the compressor duct may not suffice. In this regard, however, it is of interest to note that Mani [10] has achieved some quite reasonable comparisons with experiments using very simple representations of the system parameters.

2) Inlet flow field - A description of the upstream flow is included in the theory. The flow upstream of the compressor is modeled as two-dimensional and unsteady, but irrotational. The upstream annulus is taken as having constant area. This assumption can readily be relaxed, if

necessary. It is not clear how valid the irrotationality assumption is, and this is a subject for investigation. Data is scarce on this point, although the comments of Day do give credence to this assumption.

Perhaps more serious is the assumption that axial and circumferential disturbances are related as they would be if they were harmonic. This assumption requires study and evaluation. Also, it has been assumed that entrance to the inlet guide vane is accomplished without local head loss.

3) Exit flow field - A description of the exit flow field is included in the theory. A more important assumption is that of linearity in the exit pressure perturbations. It is clear that this cannot be correct, in general, although the degree to which it is in error and, more importantly, its effect on the predictions of the theory is not clear. Previous theories of steady-state rotating stall, in particular [3] and [11] which have made this assumption, have had good success with predicting at least some of the features of the stall cell flow field.

4) The model of the throttle characteristic that is included is quite adequate for low pressure ratios. For higher pressure ratio systems, there will be no problem with introducing a compressible version of this, as was done by Wenzel [12].

5) Throttle transients (e.g., ramp closures) have not been included. However there should be no difficulty in applying the theory to account for these. This is of interest since it has been found that throttle transients can have a significant effect on system behavior.

6) System hysteresis is included in the theory. This appears naturally since it is set by the stability of the system at the various intersection

points of throttle and compressor curves. When closing the throttle (into stall) the compressor curve is the axisymmetric one. When opening the throttle from operation in fully developed rotating stall, the compressor curve is the rotating stall one, and there can thus be a difference in the throttle settings at which transition from unstall to stall and from stall to unstall occur.

7) Compressor geometry is represented by the axisymmetric characteristic.

8) Unsteady blade row response (internal aerodynamic lag of the compressor) is included in the theory. It is done in a rudimentary manner, because at present one does not know how much detail is needed to provide a satisfactory description.

From the above it does appear that all of the elements that one might think necessary for an analytical description of general post-stall transients have been included. Having said this, however, it should be emphasized that their inclusion has, in some instances, been done in a quite approximate manner, with an impact on the overall prediction which is not well understood. In this connection, we can refer back to the basic analysis [3] from which this study begins. The equations developed there will always result in axial velocity profiles that are like those shown in Fig. 3.4, for example. They will not yield the "top hat" type of profile that seems to be more characteristic of compressors that operate in rotating stall. At present, the reason for this discrepancy is unclear, but the fact that it exists suggests that there are aspects of the theory which should be improved, even for low speed, low pressure-ratio situations.

We have described those features that are included, and we now turn

to those that have not been, but which we think will be important to include for problems of practical interest.

1) Effects of compressibility on compressor performance and inlet and exit flow fields.
2) Front-to-rear mismatching effects due to off-design operation in the compressor.
3) Heat addition in the burner.
4) Effects of inlet flow distortion on post-stall transients.
5) Engine matching effects (non-constant speed, for example).
6) Other compression system components.
7) Steady-state hysteresis in the axisymmetric compressor characteristic, if such exists.

Research is necessary to elucidate the influence of the effects named above. In addition to these, however, there are other topics that must be explored if one is to improve the quantitative capabilities of the theory. The first of these is the development of more exact methods for the calculations. The numerical results given in the present report are based on the one-term Galerkin procedure; as mentioned, this was all that could be carried out in the limited time available. In particular, the type of phenomena that are being investigated would appear to be very well-suited for use of spectral method calculations. Such procedures would be able to directly use any Fourier series representations of the inlet and exit flow fields that are developed. At present, we are examining ways to carry out this calculation, and so we will only mention that this is one item that should be addressed.

Another item is concerned with the rotating stall performance. The question of the behavior of the compressor at or near the point of instability is by no means settled. The present theoretical analysis predicts that the flow in the compressor will become unstable at the peak of the steady-state pressure rise curve. In practice, compressors are observed to become unstable on the negatively sloped part of the curve. While interstage (one-dimensional), volume effects have been invoked to account for this in high pressure ratio compressors, this is observed at low pressure ratios also, and here the interstage effects are very small. Research is needed on this topic, both of an experimental as well as a theoretical nature.

The effect of inlet conditions has been mentioned before, and the point will not be belabored here. We will merely note that this is a new aspect of the problem, and one on which there is little data.

Effects of initial disturbance features on the subsequent transients have received only cursory attention in this report. Only a rotating-stall-like harmonic disturbance was considered, and it began when the throttle was set and held precisely at the neutral point. Obviously, a myriad of other possibilities need study; disturbances which are statistically defined fluctuations, or which arise from inlet distortions of various types, or which arise from asymmetric burner pulses, are all possibilities for transient initiation, perhaps in combination with symmetric, or surge-like, pulses arising either naturally or from control actions. Research on these questions of disturbance initiation should be helpful to guide experimental tests.

9. SUMMARY AND CONCLUSIONS

1) An approximate theory has been developed for post-stall transients in axial compression systems.

2) The analysis includes a two-dimensional unsteady representation of the compressor flow field, together with a description of the overall dynamic response of the system. A system of three simultaneous first-order ordinary differential equations are derived, through which surge-like and rotating-stall-like oscillations are coupled.

3) Examination of the coupled equations shows that surge and rotating stall can each exist in "pure" or equilibrium form; however, rotating stall cannot evolve without inducing some surge-like unsteadiness in the process. During either equilibrium surge or rotating stall, disturbances of the other family will tend to die out; that is, "pure" modes tend to be stable.

4) Transients are examined, resulting from a specified initial disturbance. They all have unsteady mass flow through the compressor, thus including situations in which rotating stall is growing or decaying. This growth or decay is calculated, along with the instantaneous system operating point. To the authors' knowledge, this is the first time that this has been done.

5) The instantaneous rotating stall cell amplitude is found to have a significant effect on the instantaneous compressor pumping characteristic. This, in turn, affects the overall system response.

6) The theory extends previous analysis about the effect of the B parameter ($B = (U/2a_s)\sqrt{V/AL_c}$) on post-stall transients, and adds details

of the transient process; how rotating stall decays for large B, and how it settles to a fixed level when B is less than the critical value.

7) Other parameters besides B, in particular the compressor length to radius ratio ℓ_c = L/R, can also have a strong effect on the system response. A limited study shows that (for a given value of B) compressors of shorter length to radius ratio are more likely to exhibit surge than rotating stall. The initial conditions concerning stall cell amplitude at the start of the transient are presumably also of importance, and should carefully be studied.

8) The rotating-stall cell amplitude during unsteady flow is different from that during steady-state operation in rotating stall. Consequently, the instantaneous compressor performance during a system transient can differ considerably from the characteristic measured during steady-state rotating stall.

9) The numerical results that are presented show qualitative agreement with the existing (but scarce) experimental data concerning the nature of the flow field during this type of transient.

10) Based on the results of the analysis, recommendations are made concerning future work in the area of stagnation stall.

FIGURES

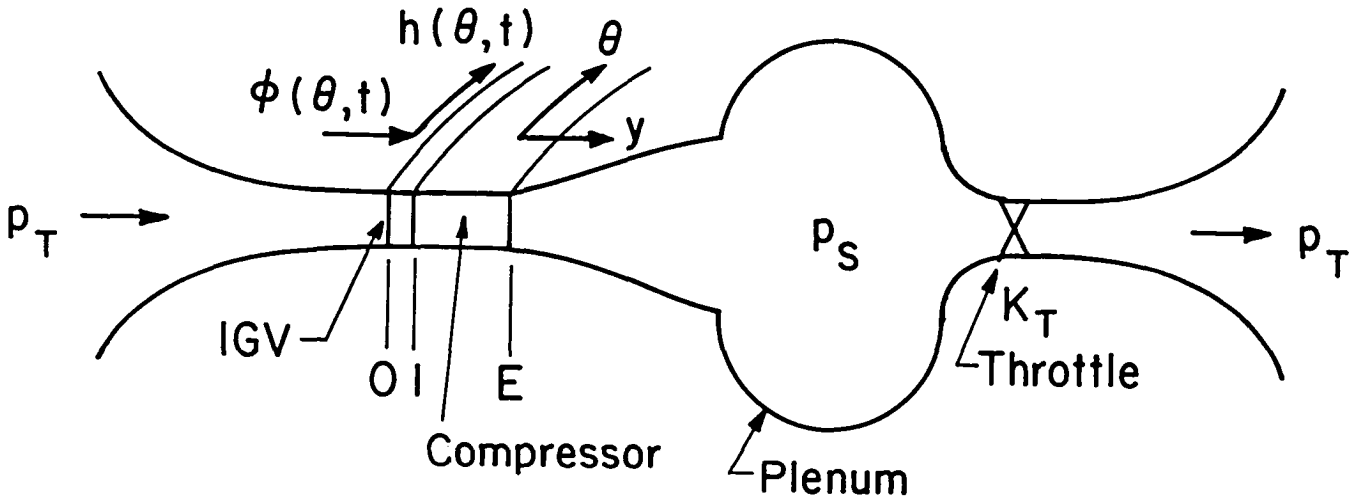

Figure 2.1 Schematic of compressor/compression system geometry.

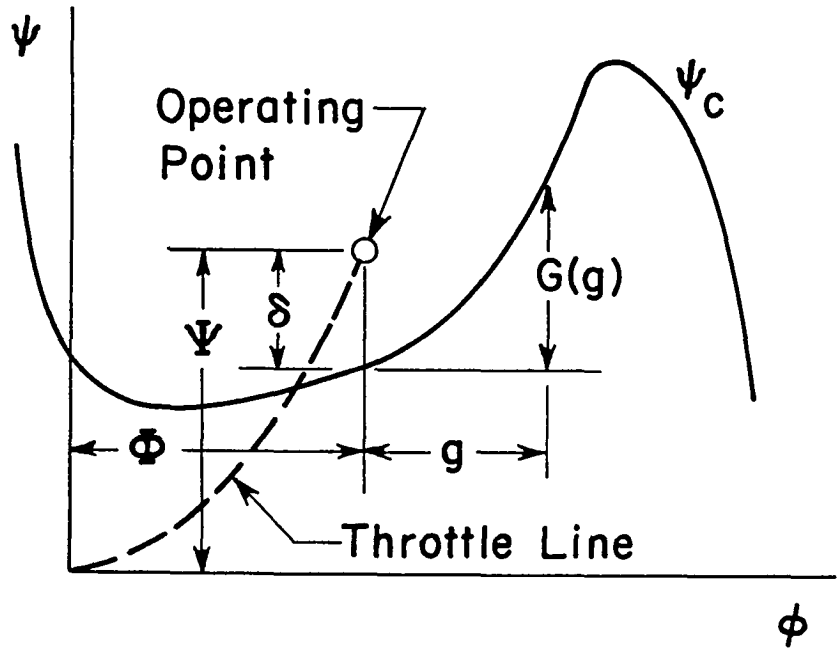

Figure 3.1 Notation used for compressor performance characteristics. Total-to-static pressure rise (ψ_c) vs. flow coefficient (ϕ) in absence of rotating stall. Operating point in rotating stall is δ above ψ_c.

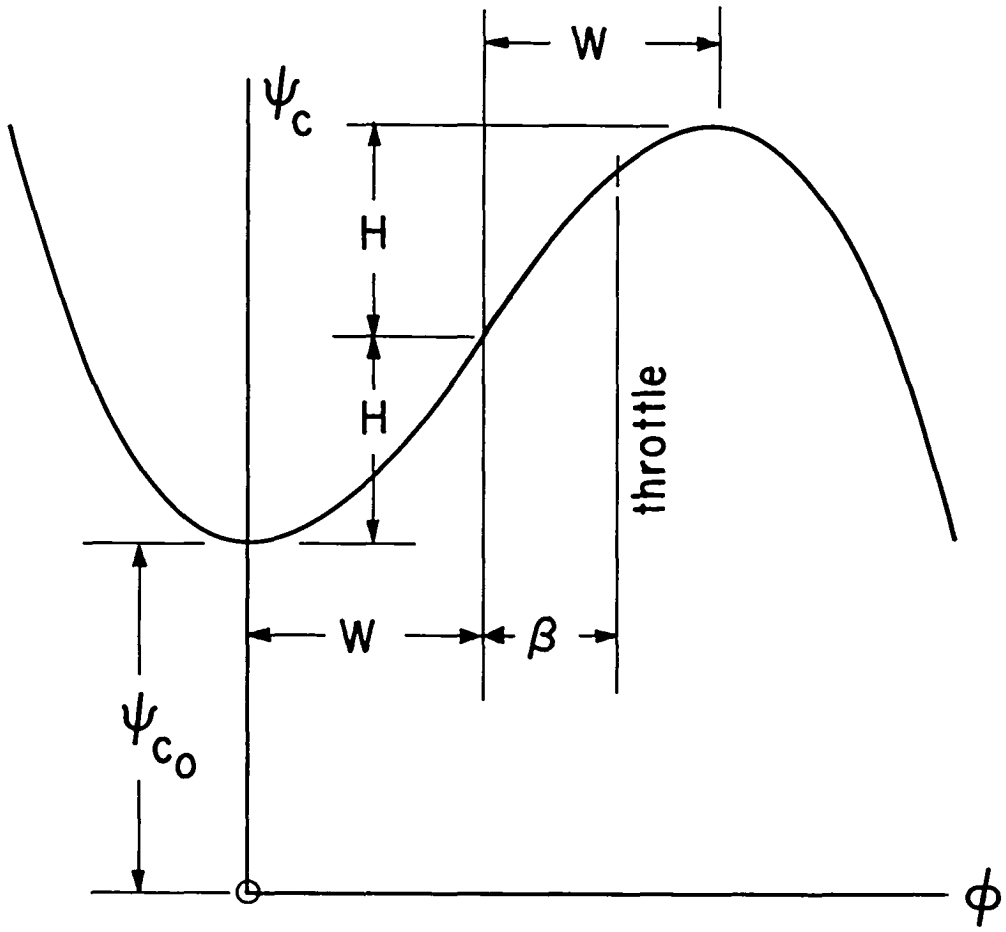

Figure 3.2 Notation used in definition of cubic axisymmetric compressor characteristic. β defines throttle setting.

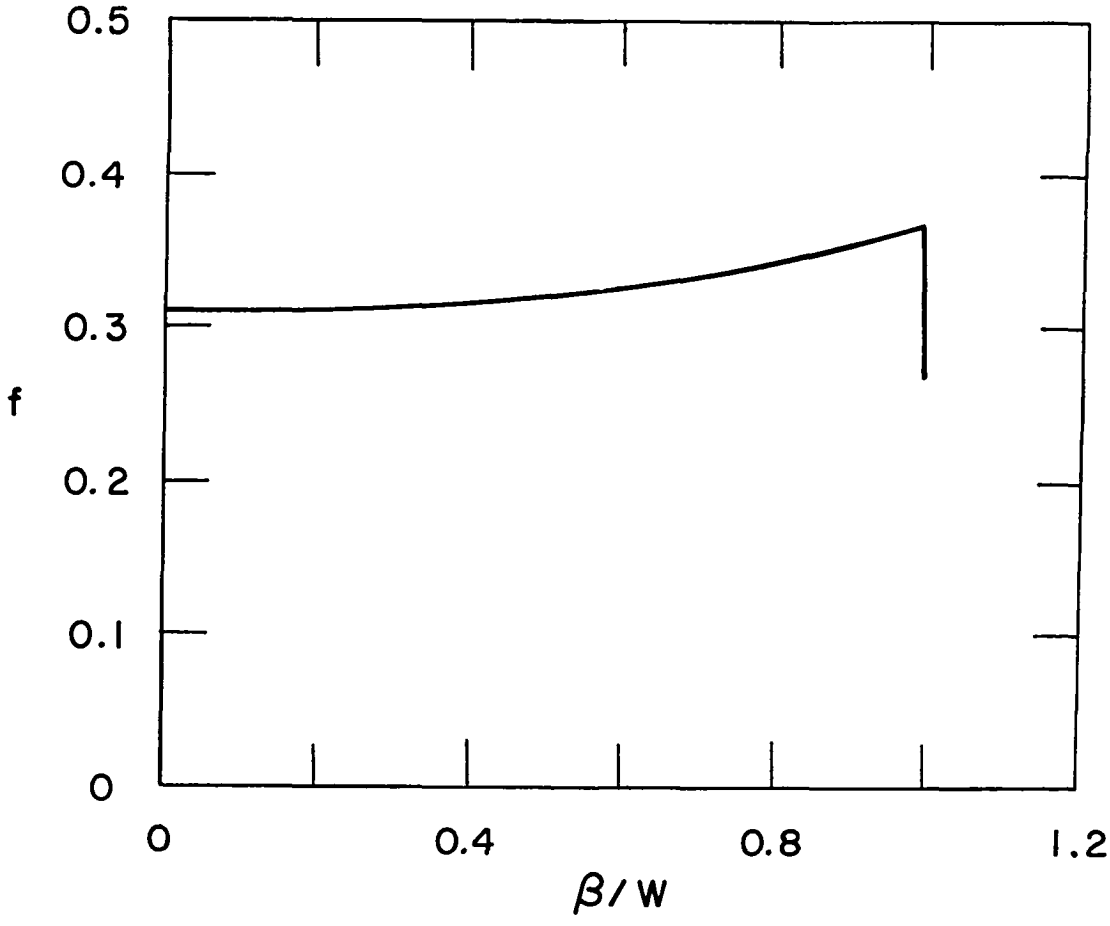

Figure 3.3 Nondimensional stall cell speed (f) vs. (normalized) throttle setting (β/W), calculated numerically for cubic characteristic with H/W = 0.72.

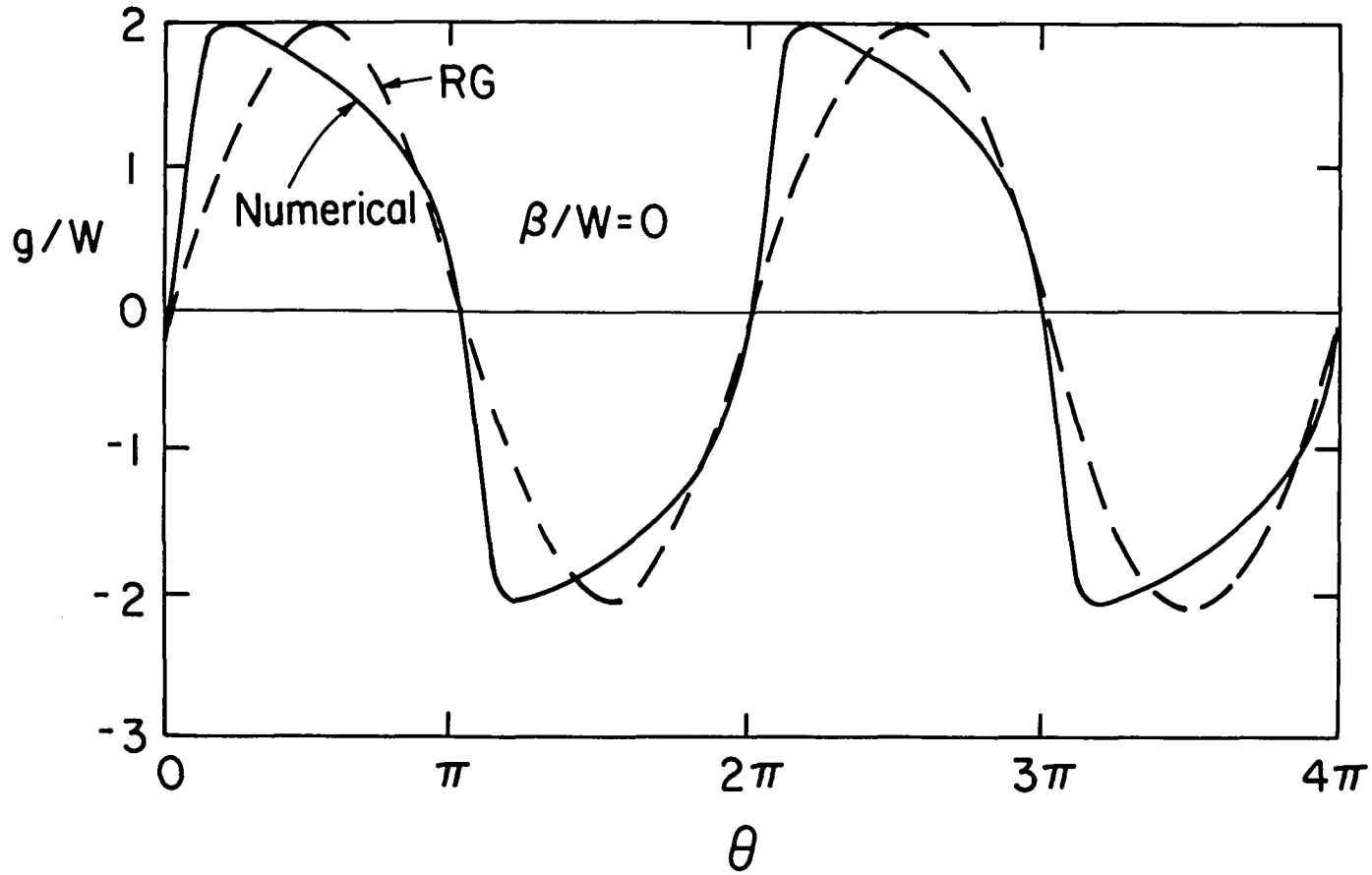

Figure 3.4(a) Comparison between numerical calculation and single harmonic Galerkin representation of axial velocity profile (g); for $\beta/W = 0$ and cubic characteristic, $H/W = 0.72$.

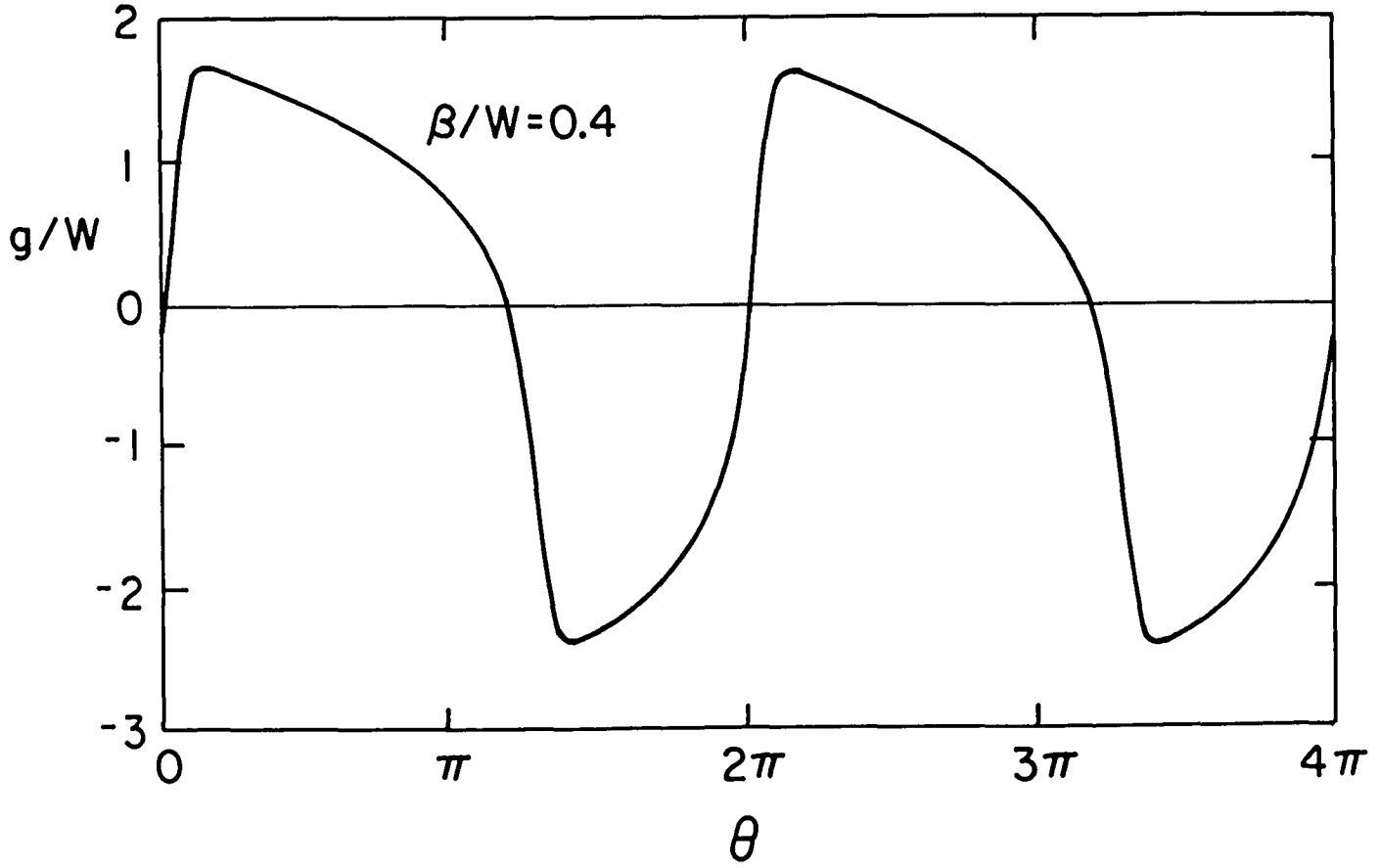

Figure 3.4(b) Numerical results for axial velocity profile; β/W = 0.4, other conditions as in (a).

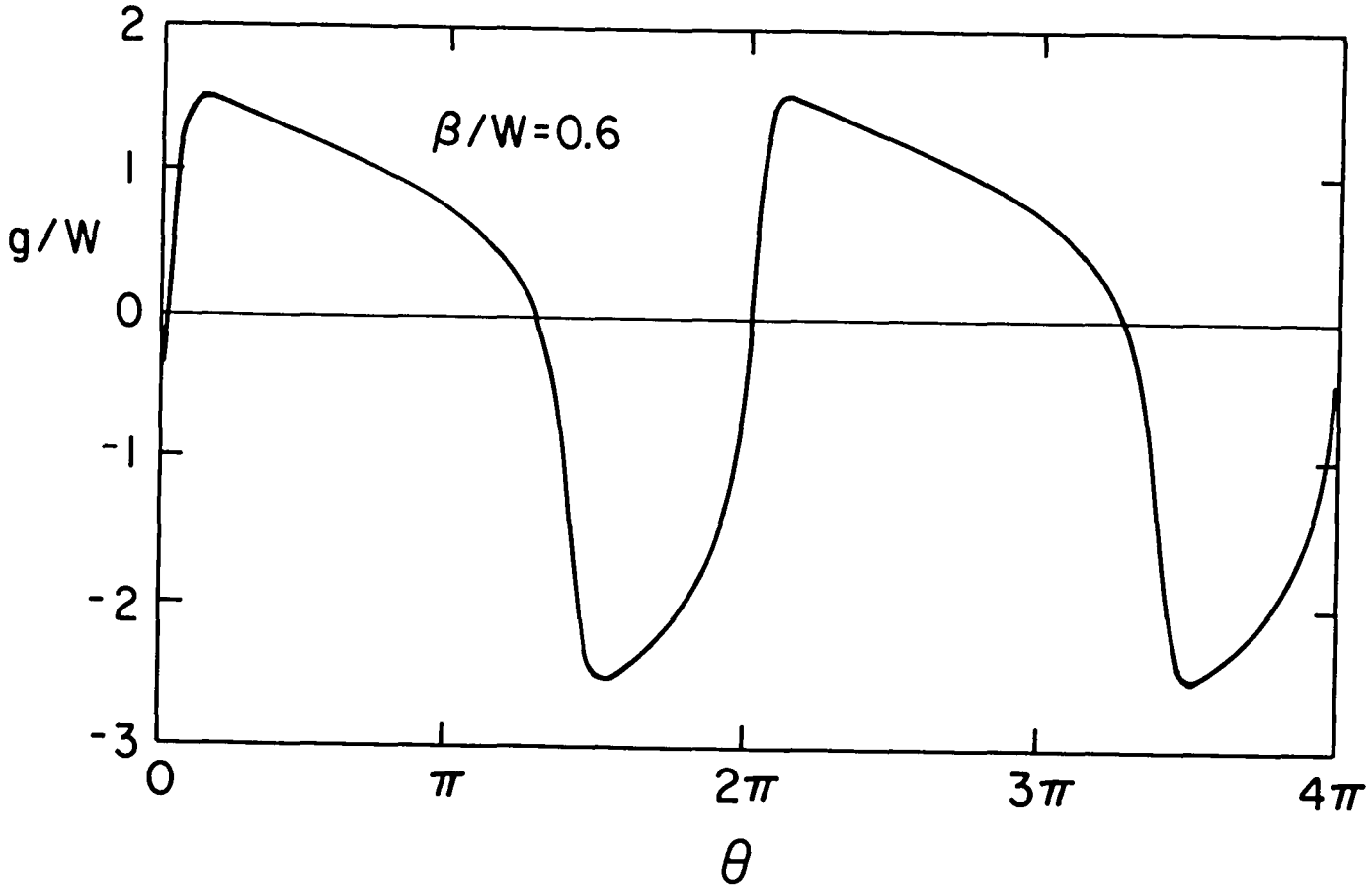

Figure 3.4(c) Numerical results for axial velocity profile; β/W = 0.6, other conditions as in (a).

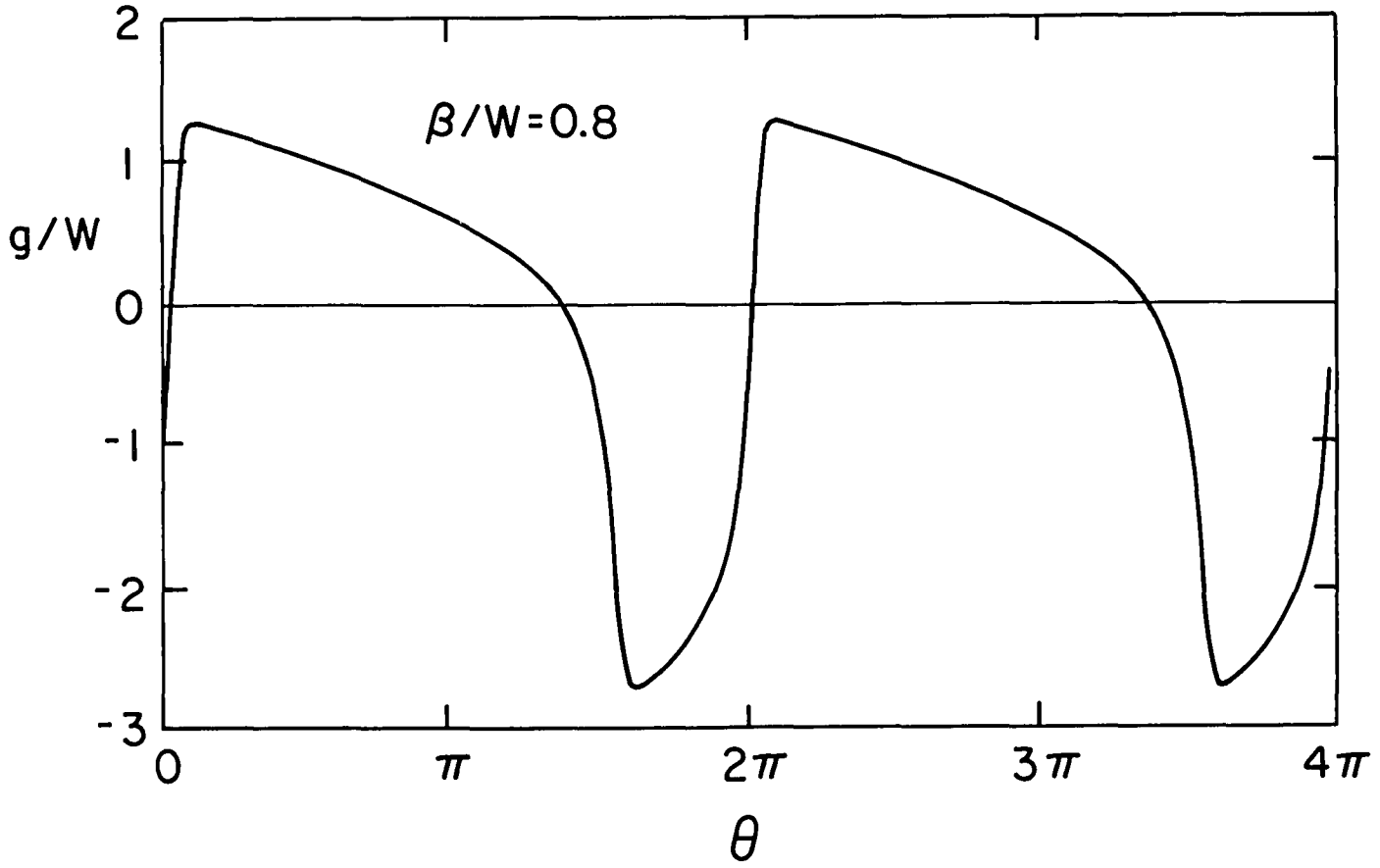

Figure 3.4(d) Numerical results for axial velocity profile; β/W = 0.8, other conditions as in (a).

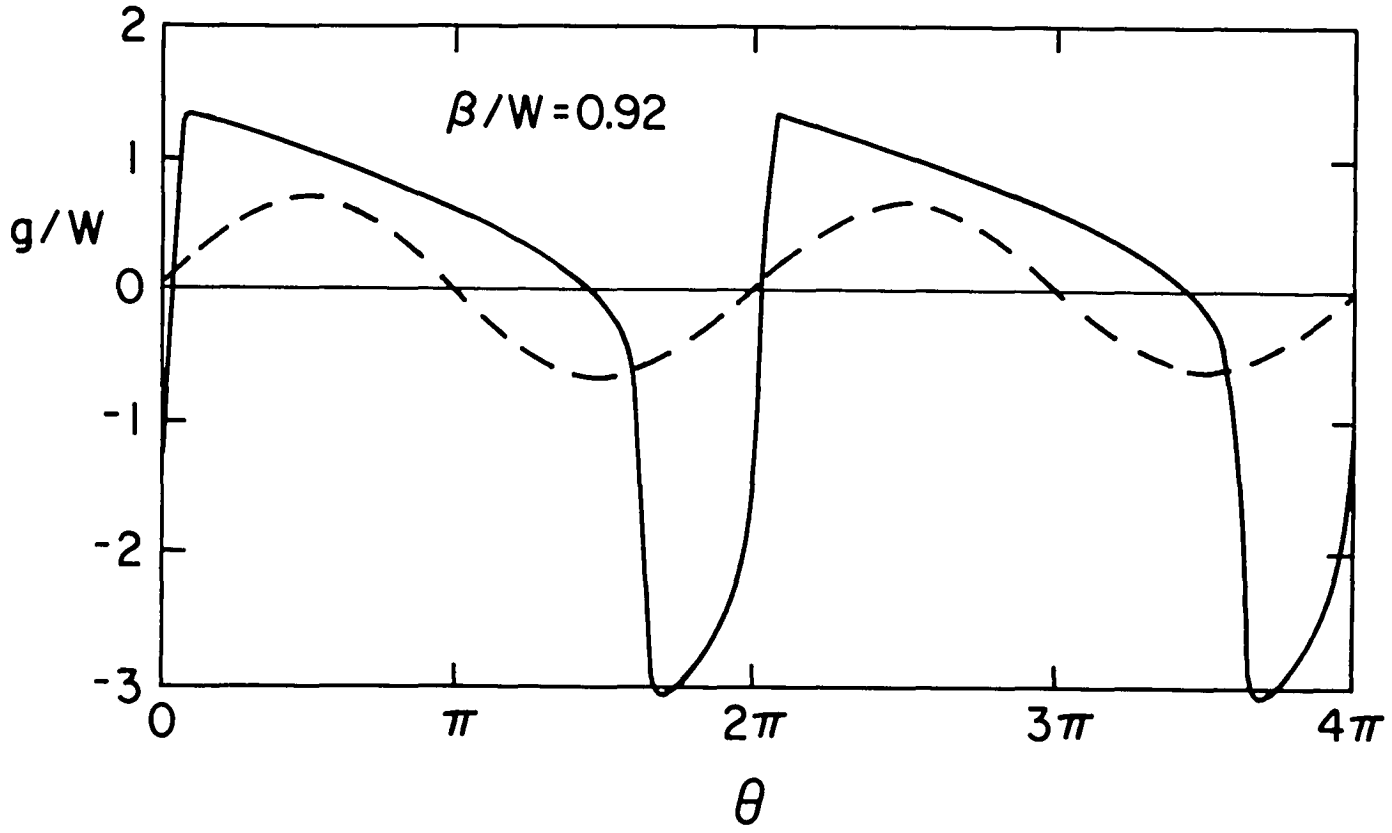

Figure 3.4(e) Comparison between numerical calculation and single harmonic Galerkin representation of axial velocity profile for $\beta/W = 0.92$, other conditions as in (a).

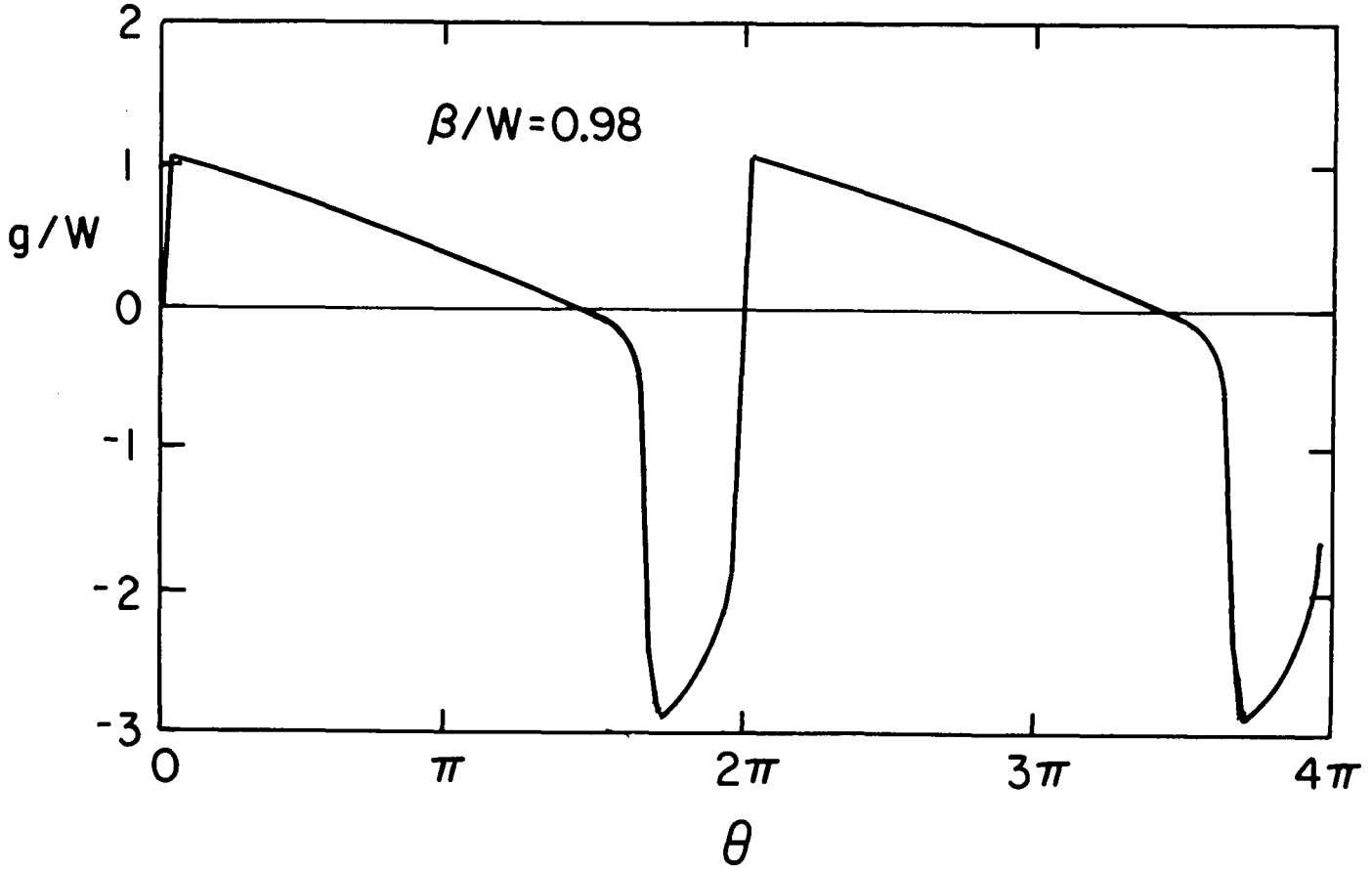

Figure 3.4(f) Numerical results for axial velocity profile; $\beta/W = 0.98$, other conditions as in (a). Note that no solution exists for $\beta/W = 1.00$.

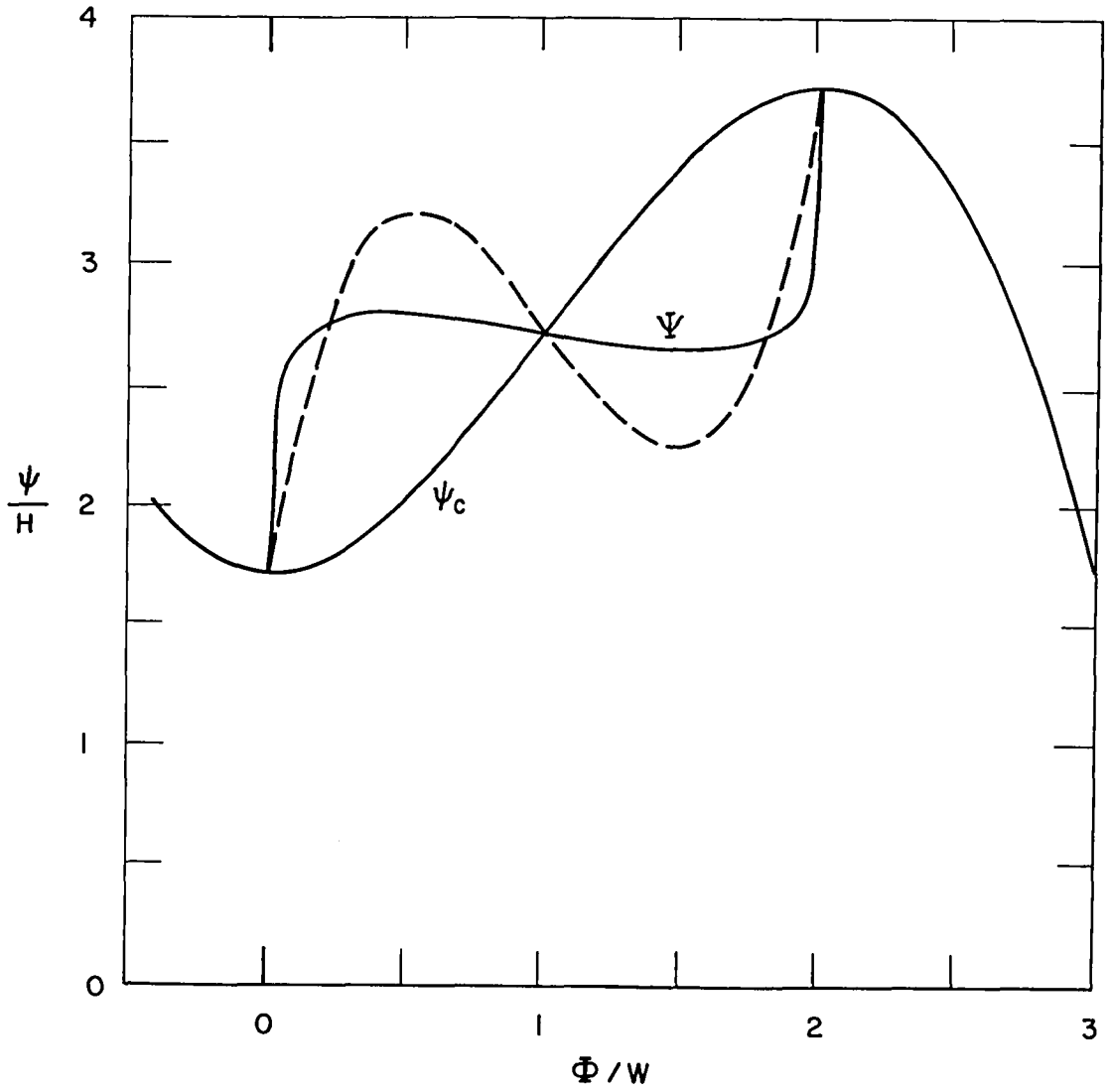

Figure 3.5 Comparison of numerical and approximate (Galerkin) solutions for calculated compressor performance (Ψ) in rotating stall; solid and dashed line respectively. Cubic axisymmetric characteristic, H/W = 0.72.

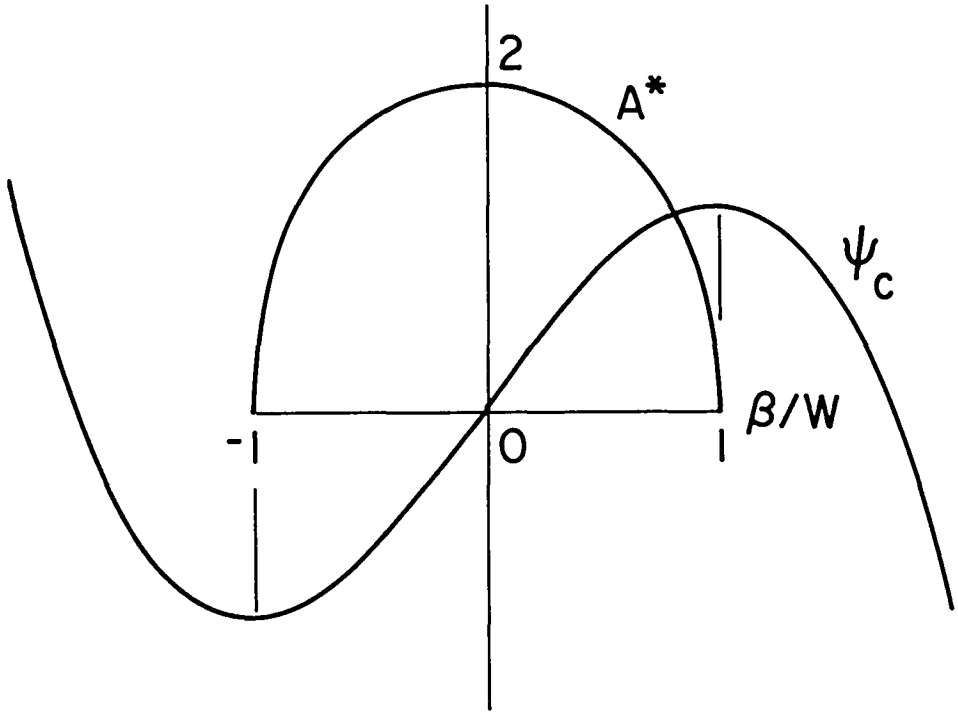

Figure 3.6 Amplitude (A*W) of single harmonic Galerkin solution as a function of β/W. The cubic axisymmetric compressor characteristic (ψ_c) is also shown for reference.

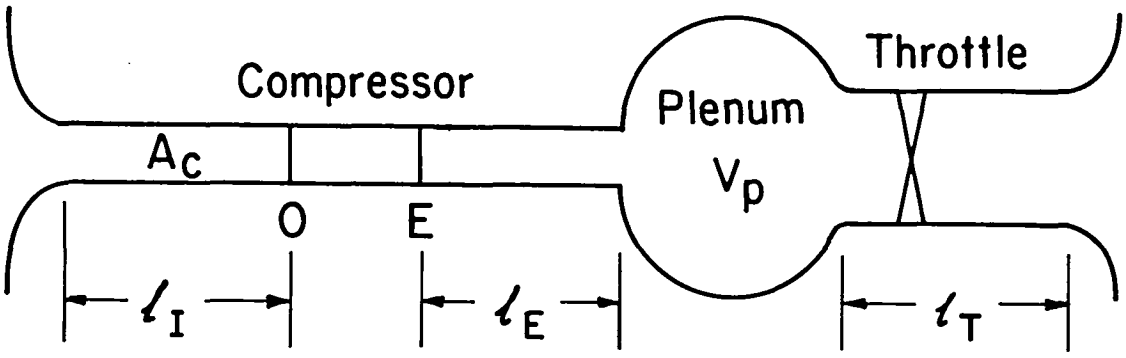

Figure 5.1 Schematic of compression system showing nondimensional lengths.

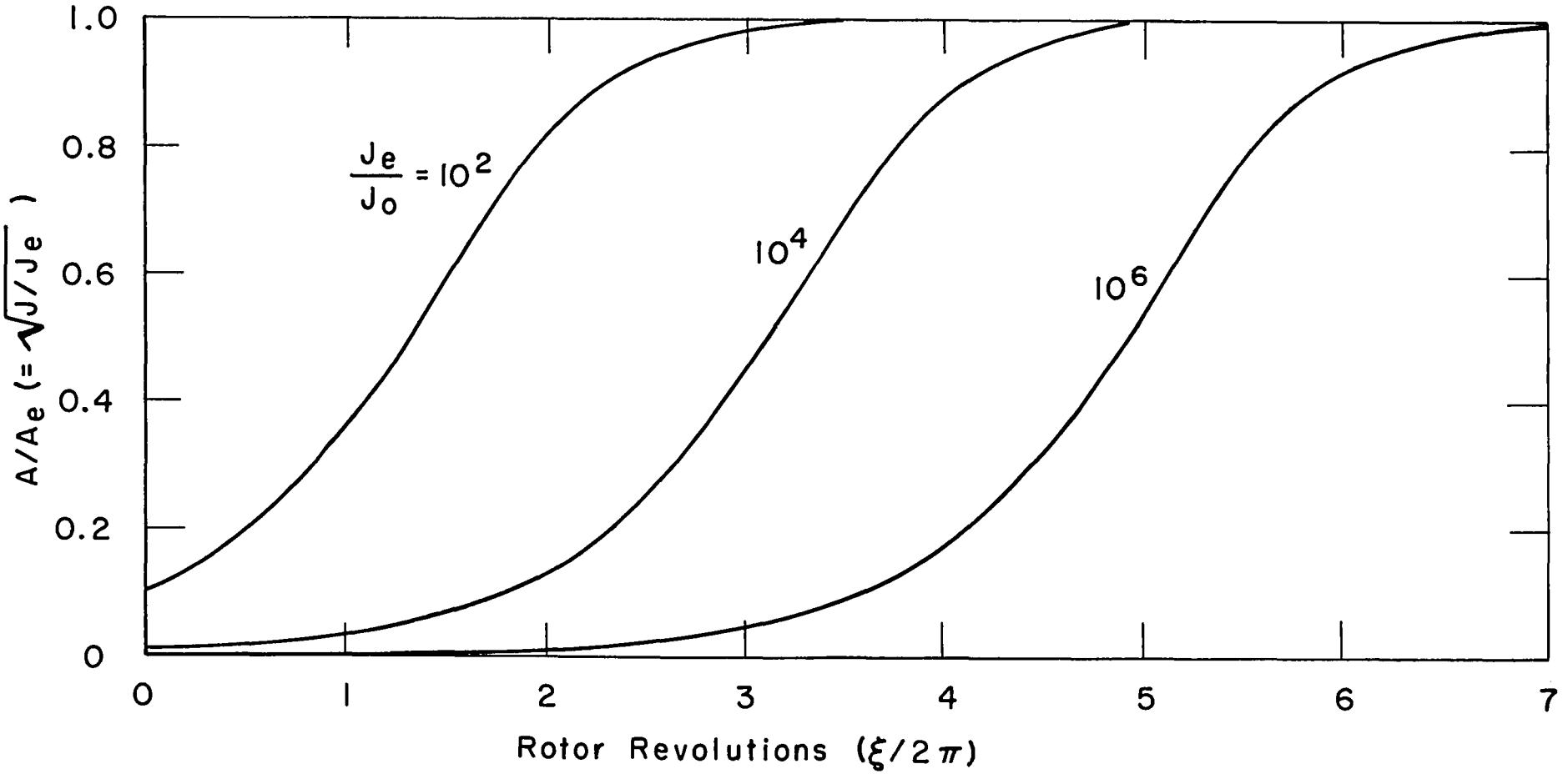

Figure 6.1 Growth of (normalized) stall cell amplitude at constant mass flow (m = 1.75, H/W = 0.72, 1/a = 3.5); curves from Eq. (6.2).

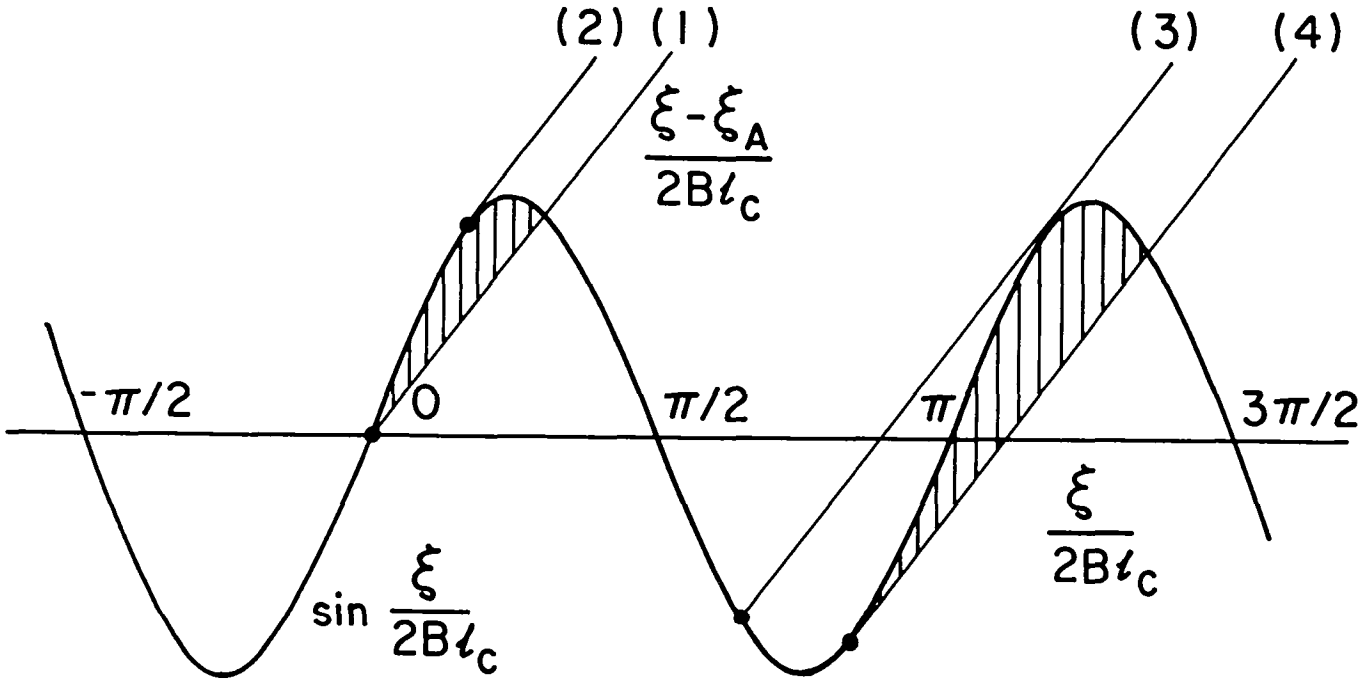

Figure 6.2 Amplitude of rotating stall during a surge cycle, as indicated by terms in Eq. (6.9), with $\beta = 0$. Different choices of ξ_A provide different starting points. Net amplification occurs in shaded zone.

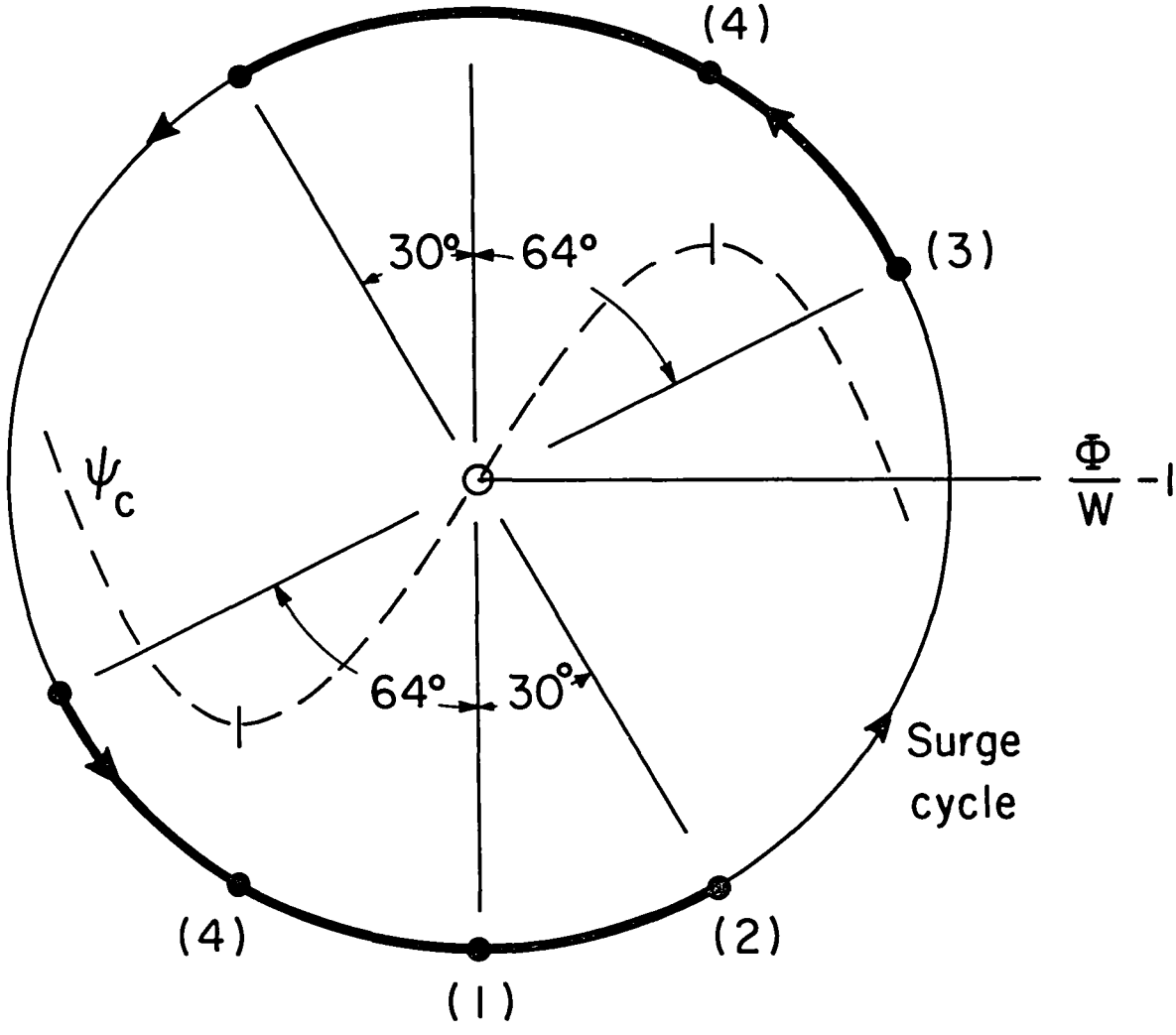

Figure 6.3 Sketch of surge cycle showing regions in which growth of rotating stall can occur. Numbered points correspond to lines of Figure 6.2.

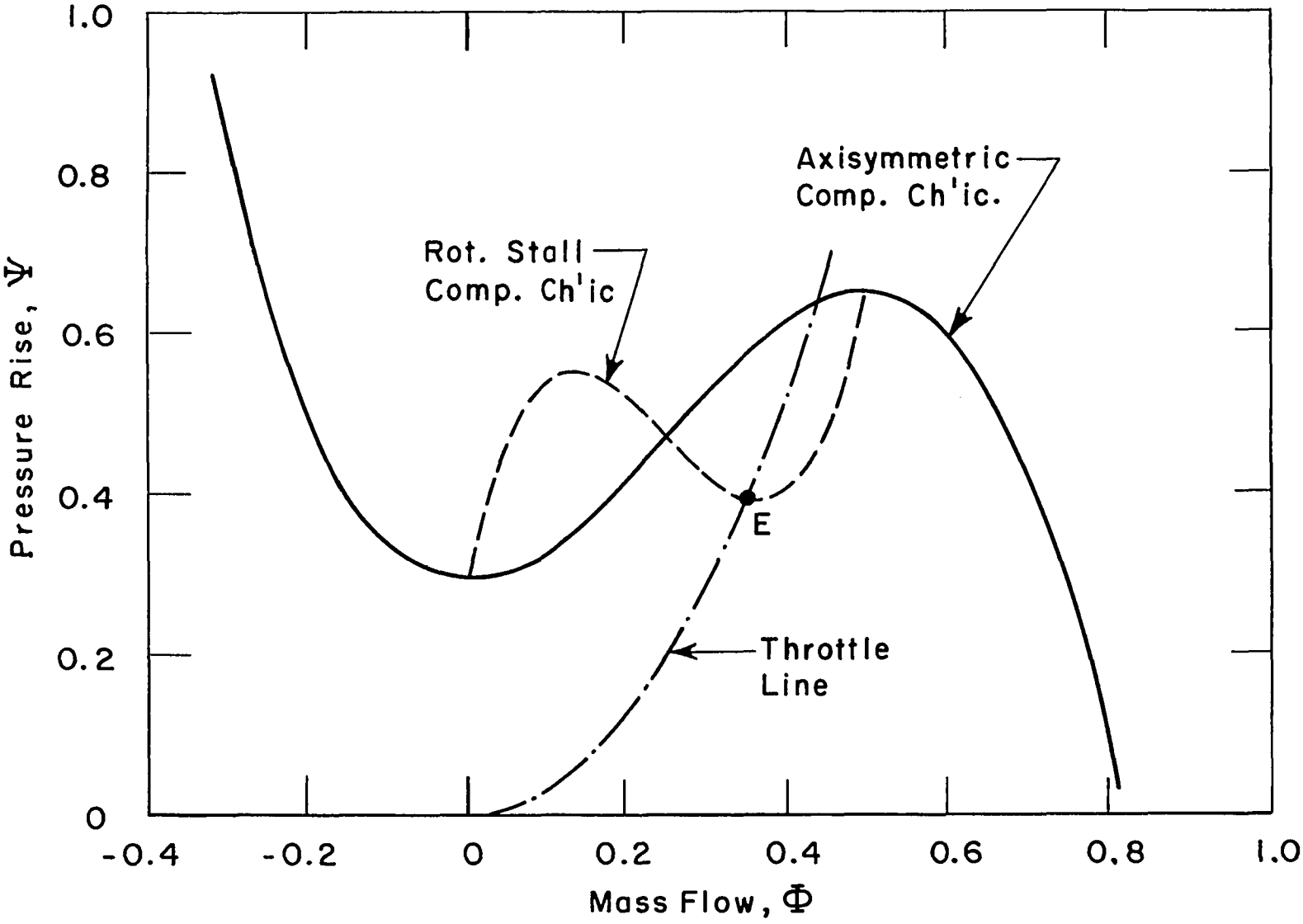

Figure 7.1 Compressor and throttle characteristics.

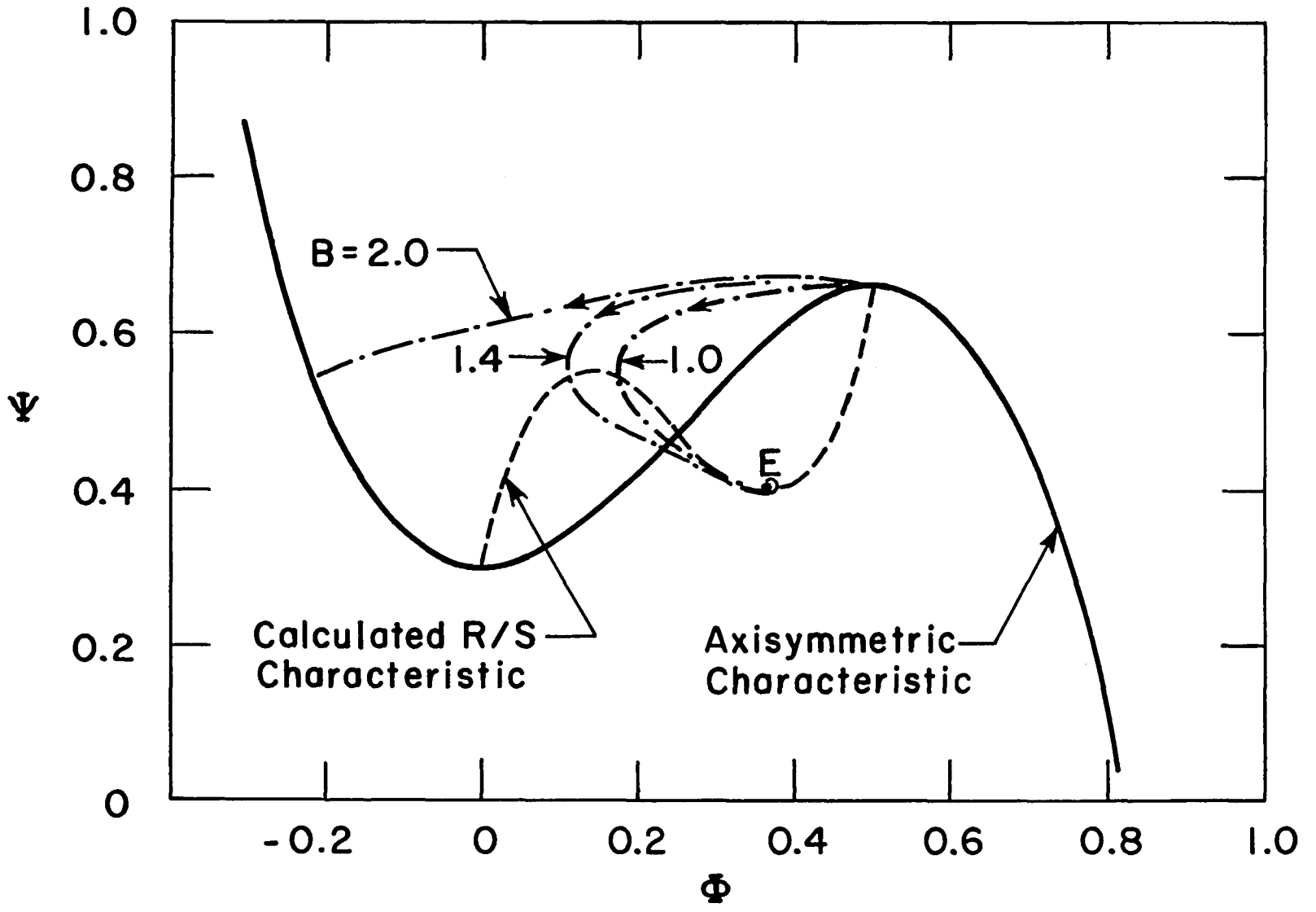

Figure 7.2 Transient compression system response (Ψ vs. Φ) for different values of B, (ℓ_c = 8.0, A(O)W = 0.005).

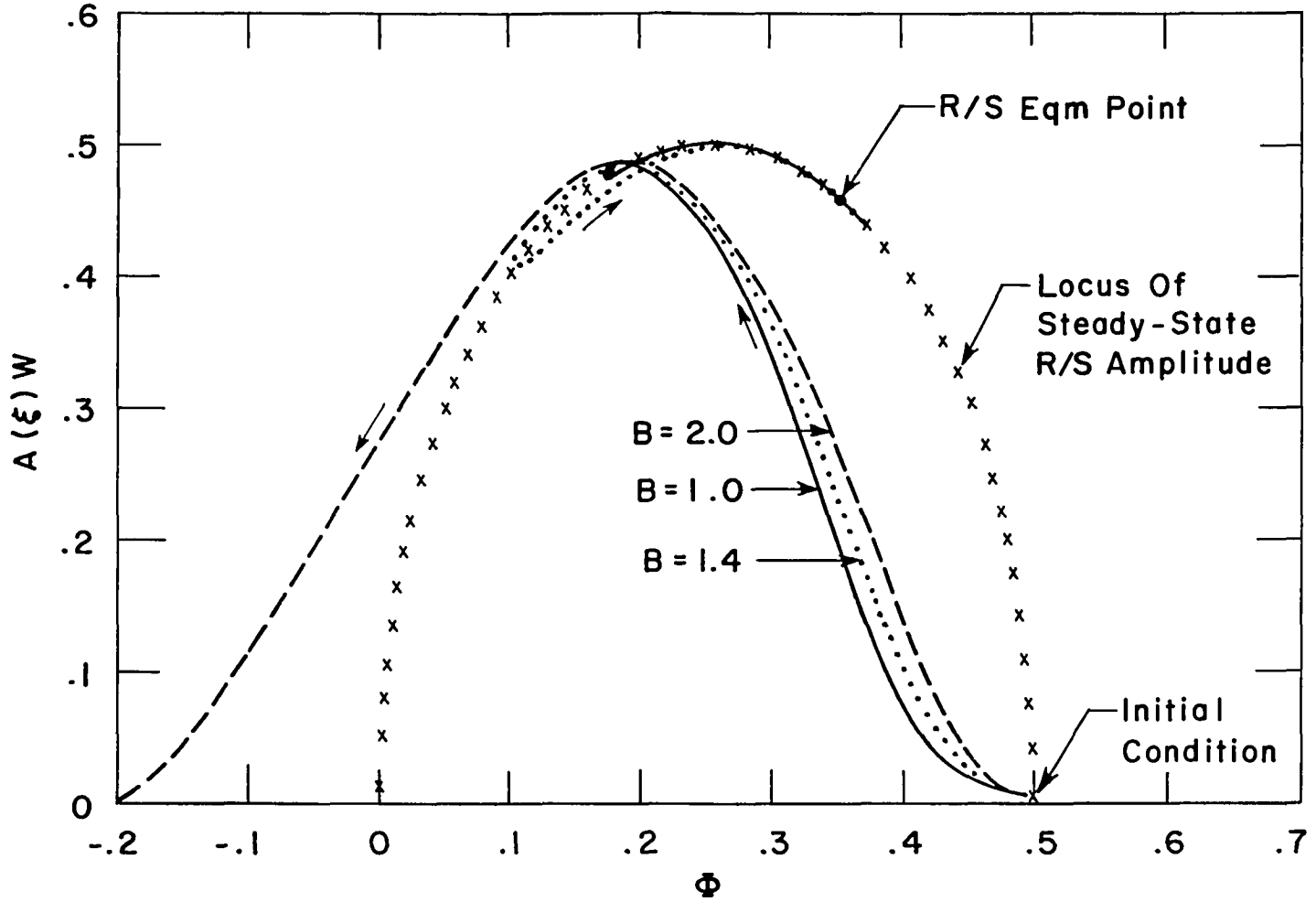

Figure 7.3 Evolution of rotating stall amplitude during system transient - effect of B parameter; stall cell ~ $A(\xi)W\sin(\theta - f\xi)$ (ℓ_c = 8.0, A(0)W = 0.005).

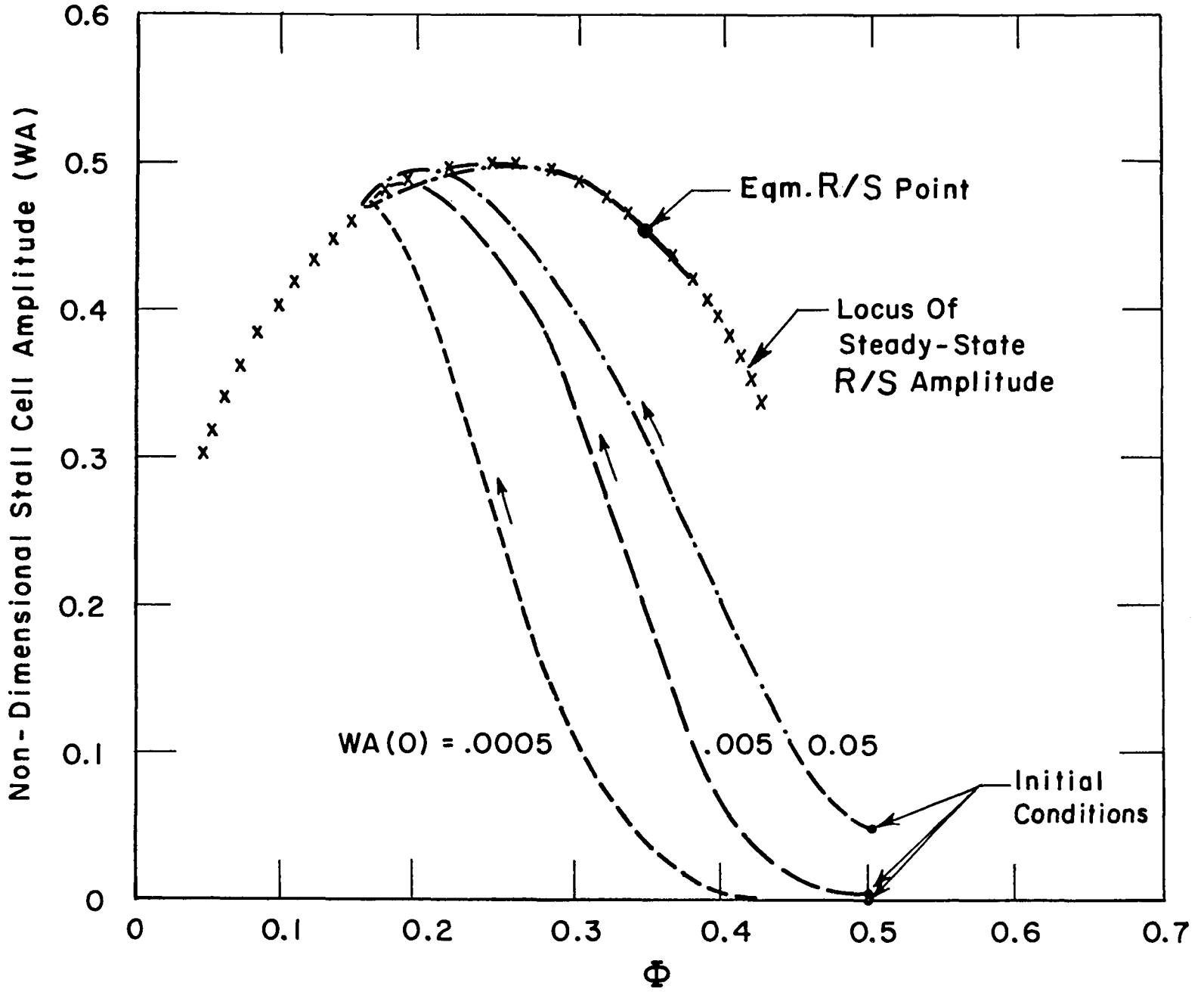

Figure 7.4 Evolution of rotating stall amplitude during system transient - effect of initial conditions; stall cell ~ $A(\xi)W\sin(\theta-f\xi)$, (ℓ_c = 8.0, B = 1.0).

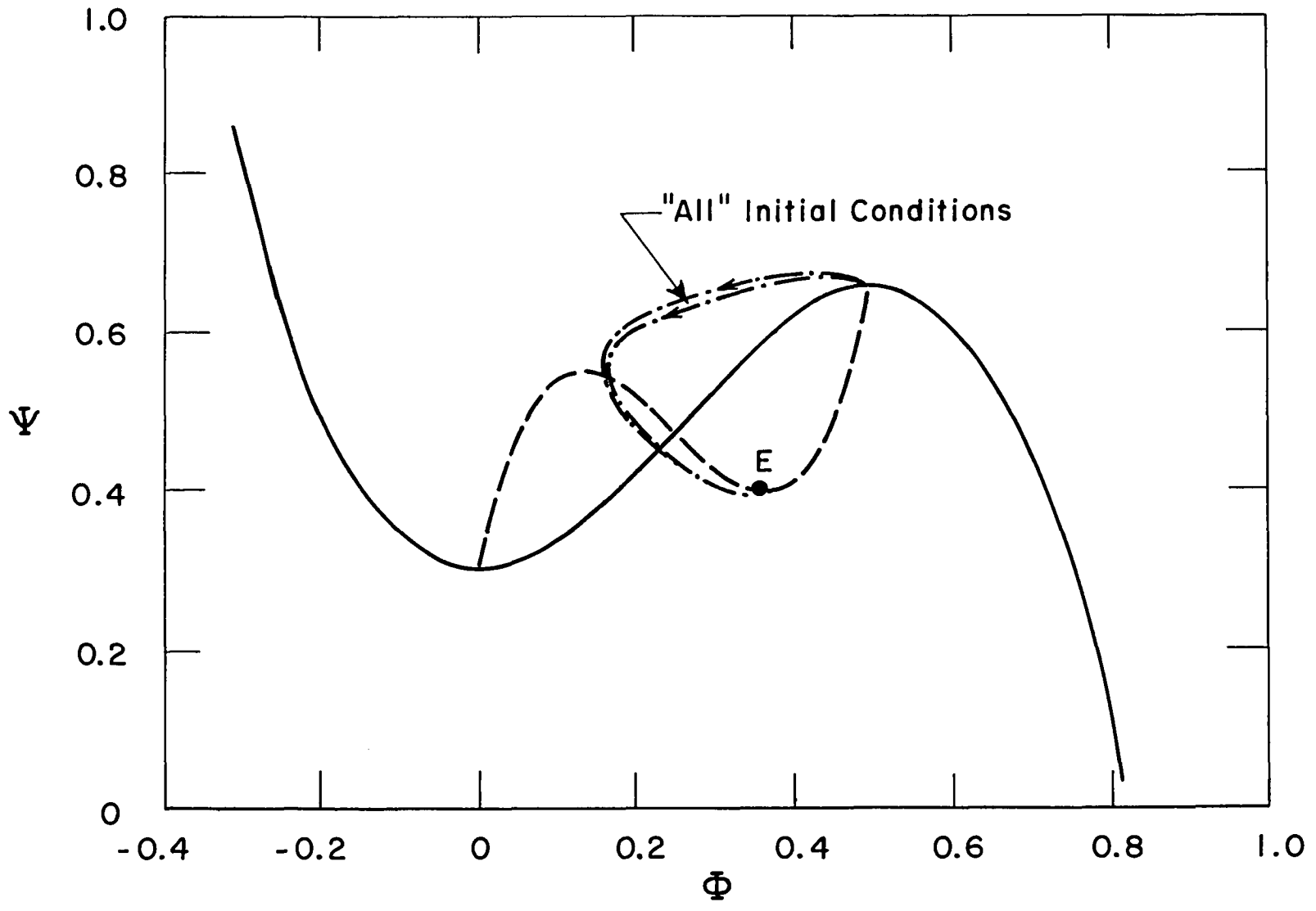

Figure 7.5 Transient compression system response - effect of initial conditions (ℓ_c = 8.0, B = 1.0).

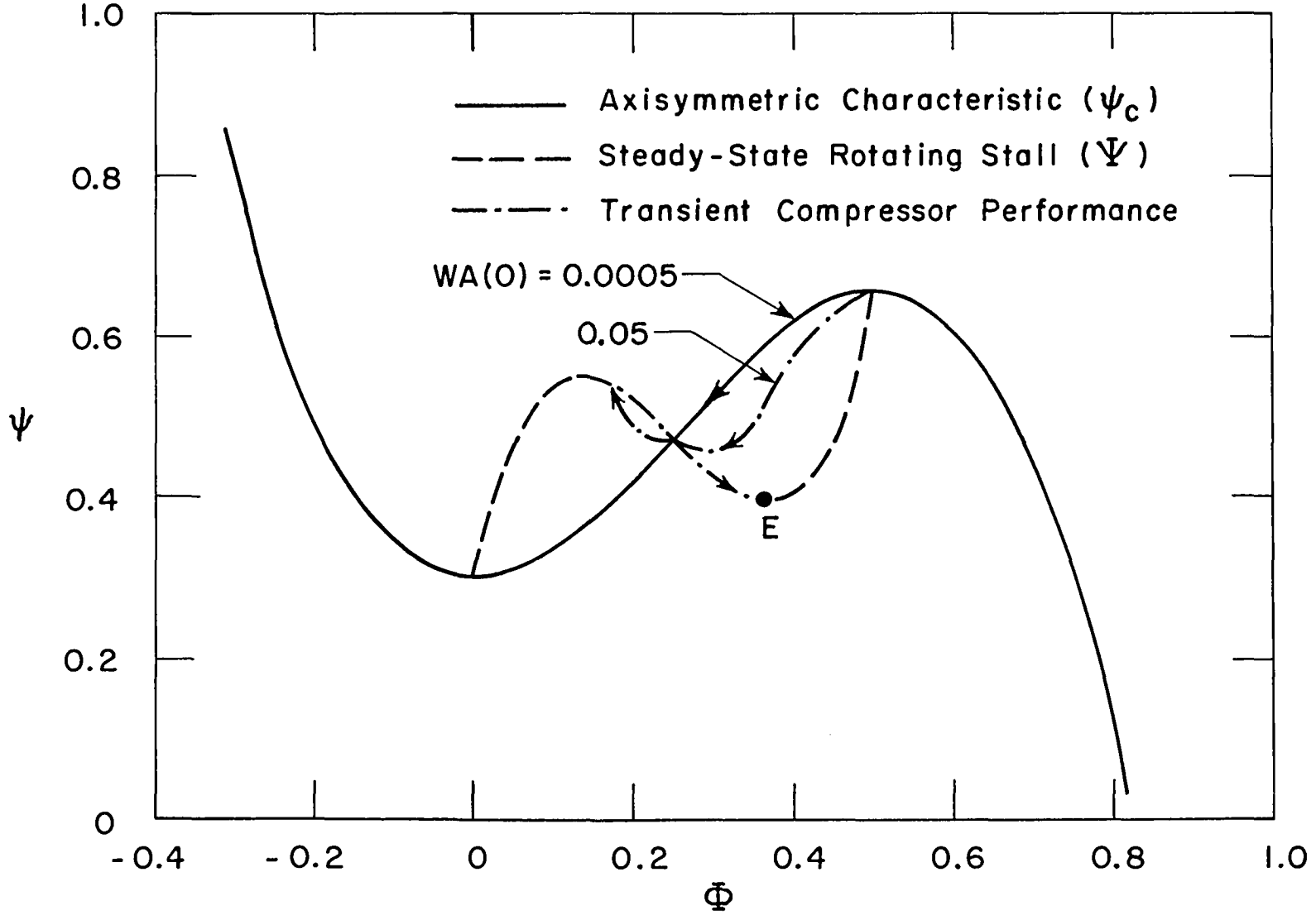

Figure 7.6 Instantaneous compressor pumping characteristic during system transient - effect of initial conditions (ℓ_c = 8.0, B = 1.0).

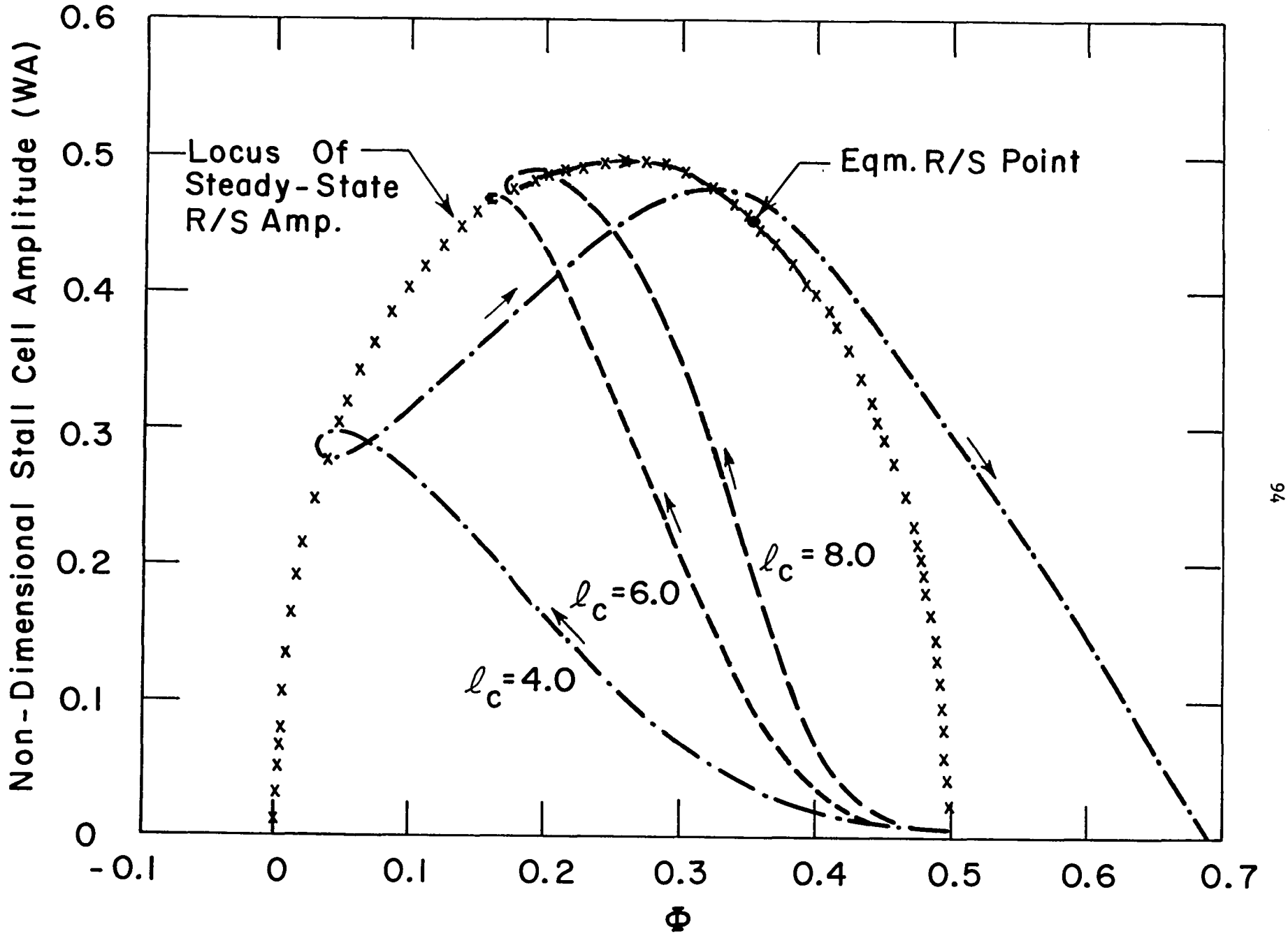

Figure 7.7 Evolution of rotating stall amplitude during system transient - effect of length-to-radius ratio; stall cell~A(ξ)Wsin(θ-fξ), (A(O)W = 0.005, B = 1.0).

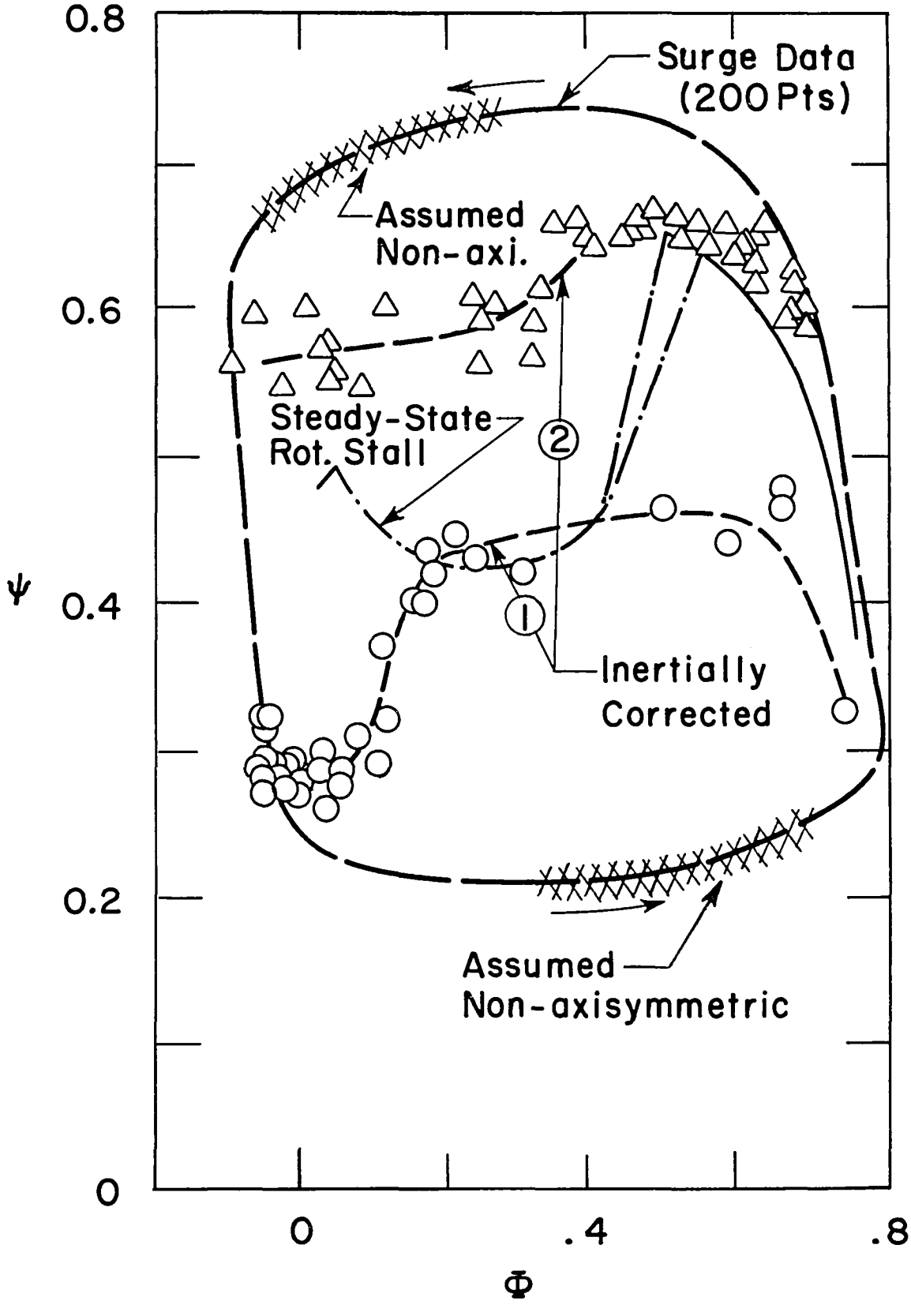

Figure 7.8 Instantaneous compressor pumping characteristic derived from surge cycle data; measured steady-state rotating stall curve also shown for reference.

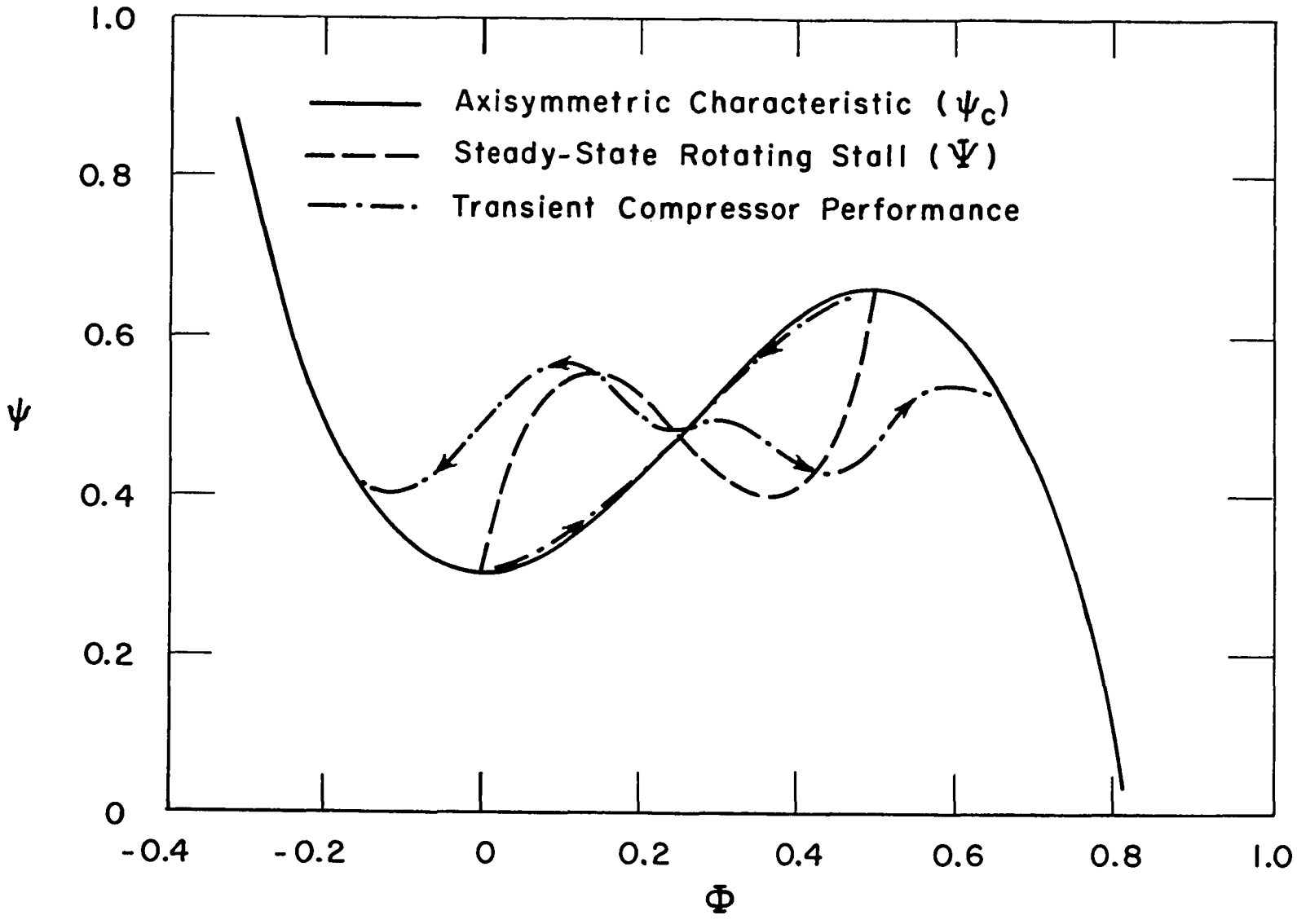

Figure 7.9 Calculated instantaneous compressor pumping characteristic (B = 1.58, ℓ_c = 8.0, A(O)W = 0.005).

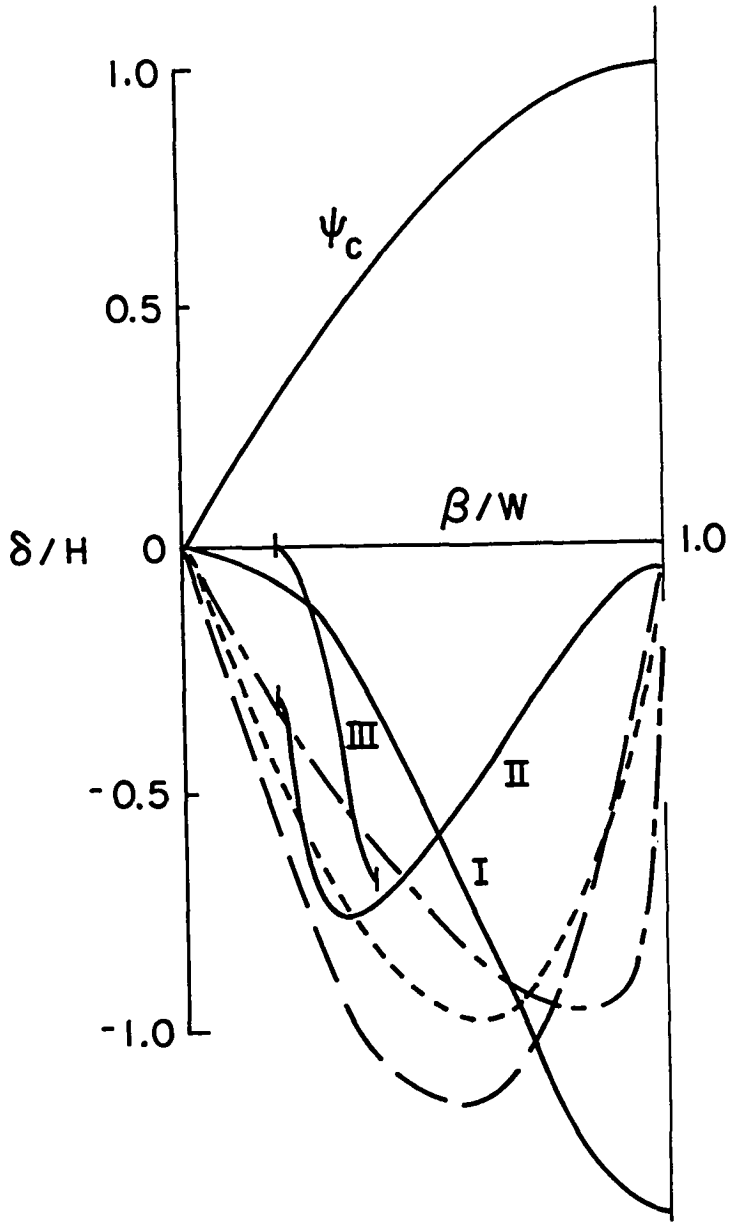

Figure B.1 Calculations of δ for numerical (dot-dash), one-harmonic Galerkin (dash), and two-harmonic Galerkin (short dash for shallow, solid for steep) diagrams. I, II, III denote three solutions for latter case.

APPENDIX A

The "dh/dθ = -g" Approximation

The relation between h and g is discussed in Ref. [3] and more fully in Appendix A of Ref. [4]. No simple exact relationships apply except in special circumstances. When the entrance duct is infinite in length and of constant width, an integral transformation connects g and h:

$$h = -\frac{1}{\pi}\int_0^{2\pi} g'(\zeta)\ell n\left|\sin\frac{\theta-\zeta}{2}\right| d\zeta \qquad (A.1)$$

Alternatively, since g(θ), being periodic, has a Fourier series of the form

$$g = \sum_{n=1}^{\infty}(a_n \sin n\theta + b_n \cos n\theta) \qquad (A.2)$$

The corresponding series for h would be

$$h = \sum_{n=1}^{\infty}(a_n \cos n\theta - b_n \sin n\theta) \qquad (A.3)$$

Eqs. (A.1) and (A.2-A.3) are equivalent. The average of g(θ) over a cycle vanishes by definition. Therefore, there is no n = 0 term in Eq. (A.2).

In Ref. [3] part II, it is shown that an exact solution (i.e., a particular set of a_n and b_n) applies when G(g) is purely parabolic, with zero slope at the throttle point g = 0. The solution may be written

$$h + ig = \hat{K}\frac{e^{i\theta}}{1 + \hat{\eta}e^{i\theta}} \qquad (A.4)$$

where $\hat{\eta}$ is an amplitude parameter.

If rotating stall oscillations have a small amplitude (Ref. [3] part I), then only the first terms of Eqs. (A.2, A.3) are needed. An obvious

example is provided by Eq. (A.4), where $\hat{\eta}$ may be set equal to 0 for small amplitude. In that case,

$$dh/d\theta = -g(\theta) \tag{A.5}$$

would be true. In Ref. [3] part III, Eq. (A.5) was used in Eq. (3.7) for limit-cycle calculations, even though it is strictly true only for weak disturbances from uniform flow.

In Appendix A of Ref. [4], it was shown that an analysis based on Eq. (A.5) may be validated for two harmonics of Eqs. (A.2, A.3): One defines a new function $z(\theta)$ as follows:

$$g \equiv -dz/d\theta \quad ; \quad h \equiv \hat{A}z - \hat{B}d^2z/d\theta^2 \tag{A.6}$$

Thus, from Eq. (A.2),

$$z(\theta) = \sum_{n=1}^{\infty} \frac{1}{n} (a_n \cos n\theta - b_n \sin n\theta)$$

and hence, Eq. (A.6) implies that

$$h = \sum_{n=1}^{\infty} (\frac{\hat{A}}{n} + n\hat{B})(a_n \cos n\theta - b_n \sin n\theta) \tag{A.7}$$

Comparing Eqs. (A.7) and (A.3), one sees that $\hat{A}$ and $\hat{B}$, until now arbitrary, may be chosen to make two harmonics agree (that is, make the first parenthesis equal to 1 for two different values of n). If, for example, the first two harmonics are to agree, then it is easily seen that

$$\hat{A} = \frac{2}{3} \quad ; \quad \hat{B} = \frac{1}{3} \tag{A.8}$$

are the proper choices.

When Eq. (A.6) is introduced into Eq. (3.7), one finds

$$(\lambda - \hat{B}mf)d^2z/d\theta^2 + mf\hat{A}z + G(-dz/d\theta) - \delta = 0 \qquad (A.9)$$

This is exactly the equation that would apply (for h instead of z) if Eq. (A.5) were used, provided λ and f are redefined. Thus, one may conclude that the approximate relation $dh/d\theta = -g$, though not exact, can be adopted for nonlinear calculations with some confidence, and we will do so in this report. We will have in mind that the procedure described by Eq. (A.6) would improve accuracy, but we leave that refinement for future studies.

APPENDIX B

Two-Harmonic Galerkin Method

In general, the Galerkin method is based on some suitable sequence of functions which, after the corresponding parameters are determined, can well represent the wave form of the oscillation. If the sequence is taken to be harmonic, of the following form, in which amplitudes have been scaled with the diagram semi-width W:

$$g = WA^* \sin\theta + WB^* \sin 2(\theta-\upsilon) \tag{B.1}$$

then the Galerkin procedure is identical to a method of straightforward solution by Fourier series. Here, we will carry out the harmonic analysis for pure rotating stall to second order, showing how the three unknowns A*, B*, and υ are found; the extension to higher orders will be obvious.

Using the $dh/d\theta = -g$ approximation, we find

$$h = WA^* \cos\theta + 1/2\ WB^* \cos 2(\theta-\upsilon) \tag{B.2}$$

The requirements of Eqs. (3.10) and (3.11) are automatically met by use of Eqs. (B.1) and (B.2). We note that if Eq. (A.3) were applicable instead of Eq. (A.5), then Eq. (B.2) would be replaced by

$$h = WA^* \cos\theta + WB^* \cos 2(\theta-\upsilon) \tag{B.3}$$

It remains to satisfy the differential equation, Eq. (3.9), with G specified by Eq. (3.16). Following the Galerkin procedure, we substitute Eq. (B.1), and, denoting the left side of Eq. (3.9) as $L(\theta)$, we find

$$\frac{1}{W} L(\theta) = (-\lambda + mf)A^*\sin\theta + (-4\lambda + mf)B^*\sin2(\theta-\upsilon) + \ldots$$

$$+ \frac{3H}{2W} \left(1 - \frac{\beta^2}{W^2}\right) - 2\frac{\beta}{W} [A^*\sin\theta + B^*\sin2(\theta-\upsilon) + \ldots]$$

$$- [A^*\sin\theta + B^*\sin2(\theta-\upsilon) + \ldots]^2$$

$$x [A^*\cos\theta + B^*\cos2(\theta-\upsilon) + \ldots] \qquad (B.4)$$

Then, we multiply $L(\theta)$ by the representational functions $\sin\theta$, $\cos\theta$, $\sin2\theta$, $\cos2\theta$, . . ., and require that the integrals of each of those products vanish over a cycle. To second order, we have four equations for the unknowns λ, A^*, B^*, and υ. With each step in order, two new moment equations and two new unknowns (amplitude and phase angle) are added.

Using the cubic form Eq. (3.16), and recalling that the average of g vanishes, the performance effect from Eq. (3.12) is

$$\delta = -\frac{1}{4\pi W^3} [3\beta \int_0^{2\pi} g^2 d\theta + \int_0^{2\pi} g^3 d\theta] \qquad (B.5)$$

into which the profile Eq. (B.1) may be substituted. By Eq. (3.5), the total in-stall performance Ψ is $\psi_c(\Phi) + \delta$. Eq. (3.13) with $\Phi = W + \beta$ gives

$$\Psi = \delta + \psi_{c_o} + H(1 + \frac{3}{2}\frac{\beta}{W} - \frac{1}{2}\frac{\beta^3}{W^3}) \qquad (B.6)$$

The two-harmonic analysis has been carried out, with B^*, λ, A^*, and υ found numerically from a set of nonlinear algebraic equations. This was done for a variety of values of a, H/W, and β. In addition, the effect of the $dh/d\theta' = -g$ approximation was investigated by keeping or not keeping

the factor 1/2 in Eq. (B.2).

Two helpful conclusions can be drawn from the results, namely that the wave profile $g(\theta)$ and performance effect δ are only weakly affected by the lag parameter a, and that the $dh/d\theta' = -g$ approximation is quite accurate. These results tend to support the one-harmonic analysis, in which those two features play no role at all.

The diagram steepness (H/W) is indicated to be a very important parameter, however, even though it too is absent from the one-harmonic result (except as a trivial matter of scale). The effect of H/W is best illustrated in terms of performance effect (δ), shown on Fig. B.1. There, the right side of a cubic diagram (ψ_C) is illustrated for H/W = 0.67 and 0.13, and below them are shown certain results for δ. As we already know, the one-harmonic result is the parabola, shown dashed, whatever the value of H/W. The numerical result (for H/W = 0.72) shown dot-dashed has a different shape, with a much more abrupt change near recovery. This is presumably dependent on H/W.

The two-harmonic solution for H/W = 0.13 is shown as the short-dashed line. Even for a "shallow" diagram, there is a shape change of the function $\delta(\beta)$. Of course, as H/W approaches zero, the one-harmonic result is approached as a limit. As H/W is increased beyond about 0.2, the two-harmonic result is unfortunately not unique. Of course, one does not know that the exact solution is in fact unique; however, the disjointed character of the three solutions (indicated as solid lines) for H/W = 0.67 suggests that the harmonic Galerkin method cannot be stopped at second order. Many harmonics would presumably be needed to achieve agreement

with the exact solution, whether or not the solution is truly unique.

Further attempts to find an improvement over the one-harmonic Galerkin analysis which is still relatively simple have failed. If it were purely a matter of representing the numerical profiles (Figs. 3.4a-f), then the method of matched asymptotic expansion by which Cole (Ref. [13]) treated the van der Pol problem could be effectively used. However, that method in effect assumes rapid changes ("relaxation") in parts of the wave process, and we cannot accept that feature if we wish to consider the initial growth of a rotating-stall disturbance; in that case, a single harmonic wave would correctly describe the first appearance of an oscillation. It seems that improvements beyond the one-harmonic Galerkin method will have to be numerical.

NOTATION

A amplitude function of first-harmonic angular disturbance, Eq. (5.50)

A^* amplitude of first-harmonic angular disturbance in pure rotating stall, Eq. (3.17)

$\hat{A}$ disturbance parameter, Eq. (5.33)

A_c compressor duct area

a reciprocal time-lag parameter of blade passage, Eq. (3.4)

a_n Fourier coefficient of axial flow disturbance

a_s sound speed

B $(U/2a_s)\sqrt{V/AL_c}$

B^* amplitude of second-harmonic angular disturbance in pure rotating stall, Eq. (B.2)

$\hat{B}$ disturbance parameter, Eq. (5.33)

b blade chord

b_n Fourier coefficient of axial flow disturbance

C_x axial flow velocity

D mean wheel diameter

E number of order 1, Eq. (1.5)

F pressure-rise coefficient in blade passage, Eq. (2.4)

F_T throttle characteristic function, Eq. (5.36)

F_T^{-1} inverse of throttle function

f speed coefficient, relative to laboratory, of propagation of angular disturbance

f_o value of f for harmonic-wave rotating stall, Eq. (5.55)

G compressor characteristic disturbance function, Eq. (3.6)

g disturbance of axial flow coefficient

H semi-height of cubic axisymmetric characteristic, Fig. 3.2

h circumferential velocity coefficient

J square of amplitude of angular disturbance of axial-flow coefficient, Eq. (5.57)

J_o initial value of J

J_e value of J for fully-developed rotating stall at the existing average axial-flow coefficient, Eq. (6.1)

K coefficient, Eq. (1.2)

$\hat{K}$ parameter of exact solution, Eq. (A.4)

K_G loss coefficient at IGV entrance, Eq. (5.6)

K_T parabolic throttle coefficient, Eq. (4.3)

k factor accounting for interrow spacing, Eq. (5.21)

k_T linear throttle coefficient, Eq. (4.4)

L left side of an equation; zero exactly, made to vanish on certain averages in a Galerkin method

L_c total effective length of compressor and ducts, Eq. (1.2)

L_R axial length of a blade row, Eq. (5.21)

ℓ_c total length of compressor and ducts, in wheel radii, Eq. (1.7)

ℓ_I length of entrance duct, in wheel radii, Fig. 5.1

ℓ_E length of exit duct, in wheel radii, Fig. 5.1

ℓ_T length of throttle duct, in wheel radii, Fig. 5.1

m duct-flow parameter of rotating stall, Eq. (3.2)

N number of stages of core compressor

P pressure coefficient, Eq. (5.13)

P_0 static pressure at entrance to IGV, Fig. 2.1

P_1 static pressure at entrance to core compressor, Fig. 2.1

P_E static pressure at compressor exit, Fig. 2.1

P_S static pressure at end of exit (diffuser) duct, and pressure in the plenum, Fig. 2.1

P_T total pressure ahead of entrance and following the throttle duct, Fig. 2.1

r time-dependent phase angle, Eq. (5.50)

t time

U wheel speed at mean diameter

u velocity in circumferential direction

V_P volume of plenum, Fig. 5.1

v velocity in axial direction

W semi-width of cubic characteristic, Fig. 3.2

Y disturbance potential at compressor entrance, Eq. (5.27)

$\hat{Y}$ function defined in Eq. (5.33)

y axial distance, FIg. 2.1

Z number of order 1, Eq. (1.3)

z function defined in Eq. (B.3)

β location of throttle setting, $(\bar{\Phi}/W)-1$

γ stagger angle of blades, 50% reaction

ΔP compressor pressure rise, Eq. (1.2)

δ performance effect of pure rotating stall, Eq. (3.5)

η axial distance measured in wheel radii, Eq. (2.2)

$\hat{\eta}$ parameter of exact solution, Eq. (A.4)

θ angular coordinate around wheel, Fig. 2.1

θ^* angular coordinate around wheel, following disturbance, Eq. (5.45)

λ rotating-stall parameter, Eq. (3.2)

υ phase angle defined in Eq. (B.1)

ξ time, referred to time for wheel to rotate one radian

ξ_e dimensionless time for development of equilibrium rotating stall, Eq. (6.4)

ξ_A defines time of start of angular disturbance, Eq. (6.8)

ρ density

τ coefficient of pressure-rise lag, Eq. (2.4)

τ_c flow change time scale, Eq. (1.2)

τ_e plenum emptying time, Eq. (1.5)

τ_H Helmholtz resonator time, Eq. (1.4)

τ_R rotating-stall formation time scale, Eq. (1.1)

Φ axial flow coefficient, averaged over angle; velocity divided by wheel speed

$\overline{\Phi}$ flow coefficient averaged over both angle and time

Φ_T flow coefficient of throttle duct, referred to entrance-duct area, Eq. (5.35)

ϕ axial flow coefficient C_x/U; variable in angle and time

$\tilde{\phi}$ velocity potential in entrance duct, Eq. (5.7)

$\tilde{\phi}'$ disturbance velocity potential, Eq. (5.10)

Ψ total-to-static pressure-rise coefficient, Eq. (3.2)

ψ pressure-rise coefficient, $\Delta P/\rho U^2$

ψ_c axisymmetric pressure-rise coefficient, Eq. (3.2)

ψ_{co} shut-off value of axisymmetric characteristic, Fig. 3.2

ω_H Helmholtz frequency, Eq. (1.4)

Subscripts

0 at the entrance to the compressor

E at the exit of the compressor

REFERENCES

1. Stetson, H.D., "Designing for Stability in Advanced Turbine Engines," article in AGARD CP324, Engine Handling, October 1982.

2. Day, I.J., Greitzer, E.M., and Cumpsty, N.A., "Prediction of Compressor Performance in Rotating Stall," ASME J. Eng. Power, 100, January 1978, pp. 1-14.

3. Moore, F.K., "A Theory of Rotating Stall of Multistage Compressors, Parts I, II, III," ASME J. Eng. Power, 106, April 1984, pp. 313-336.

4. Moore, F.K., "A Theory of Rotating Stall of Multistage Compressors," NASA Contractor Report 3685, July 1983.

5. Greitzer, E.M., "Surge and Rotating Stall in Axial Flow Compressors, Parts I, II," ASME J. Eng. Power, 98, April 1976, pp. 190-217.

6. Greitzer, E.M., "The Stability of Pumping Systems - the 1980 Freeman Scholar Lecture," ASME J. Fluids Eng., 103, June 1981, pp. 193-243.

7. Koff, S.G., and Greitzer, E.M., "Stalled Flow Performance for Axial Compressors - I: Axisymmetric Characteristics," ASME paper 84-GT-93, 1984.

8. Koff, S.G., "Stalled Flow Characteristics for Axial Compressors," S.M. Thesis, Massachusetts Institute of Technology, Department of Mechanical Engineering, 1983.

9. Magnus, Vibrations, chapter 3, Blackie and Sons, London, 1965.

10. Mani, R., "Compressor Post Stall Operation," Lecture Notes from AIAA Professional Study Seminar on Airbreathing Propulsion, Gordon C. Oates course director, June 1982.

11. Cumpsty, N.A. and Greitzer, E.M., "A Simple Model for Compressor Stall Cell Propagation," ASME J. Eng. Power, 104, January 1982, pp. 170-176.

12. Wenzel, L. and Bruton, W.M., "Analytical Investigation of Non-Recoverable Stall," NASA TM-82792, 1982.

13. Cole, J.D., Perturbation Methods in Applied Mathematics, chapter 2, Ginn and Company, Boston, 1968.

1. Report No.	2. Government Accession No.	3. Recipient's Catalog No.
NASA CR-3878		

4. Title and Subtitle	5. Report Date
A Theory of Post-Stall Transients in Multistage Axial Compression Systems	March 1985
	6. Performing Organization Code

7. Author(s)	8. Performing Organization Report No.
F. K. Moore and E. M. Greitzer	None
	10. Work Unit No.

9. Performing Organization Name and Address	11. Contract or Grant No.
Cornell University and Massachusetts Institute of Technology Sibley School of Mechanics Gas Turbine Laboratory and Aerospace Engineering Dept. of Aeronautics and Astronautics Grumman Hall Cambridge, Massachusetts 02139 Ithaca, New York 14853	NAG3-34 and NSG-3208
	13. Type of Report and Period Covered
12. Sponsoring Agency Name and Address	Contractor Report
National Aeronautics and Space Administration Washington, D.C. 20546	14. Sponsoring Agency Code 505-40-1A (E-2381)

15. Supplementary Notes

Final report. Project Manager, Michael J. Pierzga, Propulsion Laboratory, AVSCOM Research and Technology Laboratories, Lewis Research Center, Cleveland, Ohio 44135. F.K. Moore, Cornell University, Sibley School of Mechanics and Aerospace Engineering, Grumman Hall, Ithaca, New York 14853; E.M. Greitzer, Massachusetts Institute of Technology, Gas Turbine Laboratory, Dept. of Aeronautics and Astronautics, Cambridge, Massachusetts 02139.

16. Abstract

A theory is presented for post stall transients in multistage axial compressors. The theory leads to a set of coupled first-order ordinary differential equations capable of describing the growth and possible decay of a rotating-stall cell during a compressor mass-flow transient. These changing flow features are shown to have a significant effect on the instantaneous compressor pumping characteristic during unsteady operation, and hence on the overall system behavior. It is also found from the theory that the ultimate mode of system response, stable rotating stall or surge, depends not only on the B parameter but also on other parameters, such as the compressor length-to-diameter ratio. Small values of this latter quantity tend to favor the occurrence of surge, as do large values of B. A limited parametric study is carried out to show the impact of the different system features on transient behavior. Based on analytical and numerical results, several specific topics are suggested for future research on post-stall transients.

17. Key Words (Suggested by Author(s))	18. Distribution Statement
Rotating stall; Stall; Compressor; Instabilities; Surge	Unclassified - Unlimited STAR Category 02

19. Security Classif. (of this report)	20. Security Classif. (of this page)	21. No. of pages	22. Price*
Unclassified	Unclassified	113	A06

*For sale by the National Technical Information Service, Springfield, Virginia 22161

NASA-Langley, 1985

National Aeronautics and
Space Administration

Washington, D.C.
20546

Official Business
Penalty for Private Use, $300

THIRD-CLASS BULK RATE

Postage and Fees Paid
National Aeronautics and
Space Administration
NASA-451

POSTMASTER: If Undeliverable (Section 158
Postal Manual) Do Not Return